ISSN 2220-6124 (online)

World Journal of *Nephrology*

World J Nephrol 2018 September 7; 7(5): 96-116

Published by Baishideng Publishing Group Inc

World Journal of Nephrology

Contents

Volume 7 Number 5 September 7, 2018

ORIGINAL ARTICLE

Basic Study

ABOUT COVER

Editorial Board Member of *World Journal of Nephrology*, Jacob A Akoh, MD, Doctor, Department of Surgery, Derriford Hospital, Plymouth PL6 8DH, United Kingdom

AIM AND SCOPE

World Journal of Nephrology (*World J Nephrol*, *WJN*, online ISSN 2220-6124, DOI: 10.5527) is a peer-reviewed open access academic journal that aims to guide clinical practice and improve diagnostic and therapeutic skills of clinicians.

WJN covers topics concerning kidney development, renal regeneration, kidney tumors, therapy of renal disease, hemodialysis, peritoneal dialysis, kidney transplantation, diagnostic imaging, evidence-based medicine, epidemiology and nursing. Priority publication will be given to articles concerning diagnosis and treatment of nephrology diseases. The following aspects are covered: Clinical diagnosis, laboratory diagnosis, differential diagnosis, imaging tests, pathological diagnosis, molecular biological diagnosis, immunological diagnosis, genetic diagnosis, functional diagnostics, and physical diagnosis; and comprehensive therapy, drug therapy, surgical therapy, interventional treatment, minimally invasive therapy, and robot-assisted therapy.

We encourage authors to submit their manuscripts to *WJN*. We will give priority to manuscripts that are supported by major national and international foundations and those that are of great basic and clinical significance.

INDEXING/ABSTRACTING

World Journal of Nephrology (*WJN*) is now abstracted and indexed in PubMed, PubMed Central, China National Knowledge Infrastructure (CNKI), and Superstar Journals Database.

EDITORS FOR THIS ISSUE

Responsible Assistant Editor: *Xiang Li*
Responsible Electronic Editor: *Han Song*
Proofing Editor-in-Chief: *Lian-Sheng Ma*
Responsible Science Editor: *Ying Dou*
Proofing Editorial Office Director: *Jin-Lei Wang*

NAME OF JOURNAL
World Journal of Nephrology

ISSN
ISSN 2220-6124 (online)

LAUNCH DATE
February 6, 2012

EDITORIAL BOARD MEMBERS
All editorial board members resources online at http://www.wjgnet.com/2220-6124/editorialboard.htm

EDITORIAL OFFICE
Jin-Lei Wang, Director
World Journal of Nephrology
Baishideng Publishing Group Inc
7901 Stoneridge Drive,
Suite 501, Pleasanton, CA 94588, USA

Telephone: +1-925-2238242
Fax: +1-925-2238243
E-mail: editorialoffice@wjgnet.com
Help Desk: http://www.f6publishing.com/helpdesk
http://www.wjgnet.com

PUBLISHER
Baishideng Publishing Group Inc
7901 Stoneridge Drive,
Suite 501, Pleasanton, CA 94588, USA
Telephone: +1-925-2238242
Fax: +1-925-2238243
E-mail: bpgoffice@wjgnet.com
Help Desk: http://www.f6publishing.com/helpdesk
http://www.wjgnet.com

PUBLICATION DATE
September 7, 2018

COPYRIGHT
© 2018 Baishideng Publishing Group Inc. Articles published by this Open-Access journal are distributed under the terms of the Creative Commons Attribution Non-commercial License, which permits use, distribution, and reproduction in any medium, provided the original work is properly cited, the use is non commercial and is otherwise in compliance with the license.

SPECIAL STATEMENT
All articles published in journals owned by the Baishideng Publishing Group (BPG) represent the views and opinions of their authors, and not the views, opinions or policies of the BPG, except where otherwise explicitly indicated.

INSTRUCTIONS TO AUTHORS
http://www.wjgnet.com/bpg/gerinfo/204

ONLINE SUBMISSION
http://www.f6publishing.com

World Journal of Nephrology

Submit a Manuscript: http://www.f6publishing.com

World J Nephrol 2018 September 7; 7(5): 96-107

DOI: 10.5527/wjn.v7.i5.96

ISSN 2220-6124 (online)

ORIGINAL ARTICLE

Basic Study

A small molecule fibrokinase inhibitor in a model of fibropolycystic hepatorenal disease

Prani Paka, Brian Huang, Bin Duan, Jing-Song Li, Ping Zhou, Latha Paka, Michael A Yamin, Scott L Friedman, Itzhak D Goldberg, Prakash Narayan

Prani Paka, Brian Huang, Bin Duan, Jing-Song Li, Ping Zhou, Latha Paka, Michael A Yamin, Itzhak D Goldberg, Prakash Narayan, Department of Research and Development, Angion Biomedica Corp., Uniondale, NY 11553, United States

Scott L Friedman, Icahn School of Medicine, 1 Gustave L. Levy Place, New York, NY 10029, United States

ORCID number: Prani Paka (0000-0002-4638-8202); Brian Huang (0000-0001-8645-5142); Bin Duan (0000-0003-3302-1900); Jing-Song Li (0000-0002-7982-7152); Ping Zhou (0000-0001-9467-6834); Latha Paka (0000-0003-2795-3592); Michael A Yamin (0000-0001-6086-5047); Scott L Friedman (0000-0003-1178-6195); Itzhak D Goldberg (0000-0002-9070-6925); Prakash Narayan (0000-0002-7007-0245).

Author contributions: Narayan P, Paka P, Yamin MA, Paka L and Friedman SL substantially contributed to the conception and design of the study, acquisition, analysis and interpretation of data; Goldberg ID has contributed for funding acquisition and scientific advice; Narayan P drafted the article related to the intellectual content of the manuscript; Paka L made revisions for the reviewer's comments for the final version of the article to be published; Paka P, Huang B and Zhou P also performed *in vitro* work; Duan B and Li JS performed animal care, experimental dosing, pre and post-surgical procedures in animal models; all authors reviewed and approved the final version of the article to be published.

Institutional animal care and use committee statement: Angion's Animal Welfare Assurance # A4532-01. All the study protocols were designed to minimize pain and distress to the animals and were reviewed approved by our Angion's animal care and use committee.

Conflict-of-interest statement: Dr. Narayan reports in addition, Dr. Narayan has a patent null issued.

Data sharing statement: Angion Biomedica is a for-profit small business engaged in developing therapeutics for unmet medical needs. In keeping with corporate policy, data and research resources generated by the company are proprietary. Once all intellectual property that results from the generation of the data and research resources is protected *via* filing of patents, data and research resources generated will be made available.

ARRIVE guidelines statement: The authors have read the ARRIVE guidelines, and the manuscript was prepared and revised according to the ARRIVE guidelines.

Open-Access: This article is an open-access article which was selected by an in-house editor and fully peer-reviewed by external reviewers. It is distributed in accordance with the Creative Commons Attribution Non Commercial (CC BY-NC 4.0) license, which permits others to distribute, remix, adapt, build upon this work non-commercially, and license their derivative works on different terms, provided the original work is properly cited and the use is non-commercial. See: http://creativecommons.org/licenses/by-nc/4.0/

Manuscript source: Unsolicited manuscript

Correspondence to: Prakash Narayan, PhD, Research Scientist, Department of Research and Development, Angion Biomedica Corp., 51 Charles Lindbergh Blvd., Uniondale, NY 11553, United States. pnarayan@angion.com
Telephone: +1-516-3261200

Received: March 25, 2018
Peer-review started: March 25, 2018
First decision: April 10, 2018
Revised: July 11, 2018
Accepted: August 11, 2018
Article in press: August 11, 2018
Published online: September 7, 2018

Abstract

AIM

To evaluate the novel platelet-derived growth factor receptor and vascular endothelial growth factor receptor dual kinase inhibitor ANG3070 in a polycystic kidney

disease-congenital hepatic fibrosis model.

METHODS

At 6 wk of age, PCK rats were randomized to vehicle or ANG3070 for 4 wk. At 10 wk, 24 h urine and left kidneys were collected and rats were continued on treatment for 4 wk. At 14 wk, 24 h urine was collected, rats were sacrificed, and liver and right kidneys were collected for histological evaluation. For Western blot studies, PCK rats were treated with vehicle or ANG3070 for 7 d and sacrificed approximately 30 min after the last treatments.

RESULTS

Compared to the wild-type cohort, the PCK kidney (Vehicle cohort) exhibited a marked increase in kidney and liver mass, hepato-renal cystic volume, hepato-renal fibrosis and hepato-renal injury biomarkers. Intervention with ANG3070 in PCK rats decreased kidney weight, reduced renal cystic volume and reduced total kidney hydroxyproline, indicating significantly reduced rental interstitial fibrosis compared to the PCK-Vehicle cohort. ANG3070 treatment also mitigated several markers of kidney injury, including urinary neutrophil gelatinase-associated lipocalin, kidney injury molecule-1, cystatin C and interleukin-18 levels. In addition, this treatment attenuated key indices of renal dysfunction, including proteinuria, albuminuria and serum blood urea nitrogen and creatinine, and significantly improved renal function compared to the PCK-Vehicle cohort. ANG3070 treatment also significantly decreased liver enlargement, hepatic lesions, and liver fibrosis, and mitigated liver dysfunction compared to the PCK-Vehicle cohort.

CONCLUSION

These results suggest that ANG3070 has the potential to slow disease, and may serve as a bridge toward hepato-renal transplantation in patients with fibropolycystic disease.

Key words: Congenital hepatic fibrosis; Cyst; Fibrosis; Autosomal recessive polycystic kidney disease; Kidney; Liver; Therapy

© The Author(s) 2018. Published by Baishideng Publishing Group Inc. All rights reserved.

Core tip: In autosomal recessive polycystic kidney disease (ARPKD)-congenital hepatic fibrosis (CHF), a genetically acquired and congenital disease, approximately 20-30% of affected patients succumb within the first 1-2 mo of life, with pulmonary insufficiency secondary to renal enlargement as the primary cause of death. For children, nephrectomy and dialysis or kidney liver transplant is often warranted by approximately ten years of age. Other than transplantation, there is no cure for ARPKD-CHF. We report that platelet-derived growth factor and vascular endothelial growth factor are the intermediaries between the cystic and fibrotic components of progressive fibropolycystic disease and ANG3070, a novel dual kinase inhibitor therapy that may serve as an interesting bridge toward hepato-renal transplantation in patients with ARPKD-CHF.

Paka P, Huang B, Duan B, Li JS, Zhou P, Paka L, Yamin MA, Friedman SL, Goldberg ID, Narayan P. A small molecule fibrokinase inhibitor in a model of fibropolycystic hepatorenal disease. *World J Nephrol* 2018; 7(5): 96-107 Available from: URL: http://www.wjgnet.com/2220-6124/full/v7/i5/96.htm DOI: http://dx.doi.org/10.5527/wjn.v7.i5.96

INTRODUCTION

The highly aggressive fibropolycystic disease, autosomal recessive polycystic kidney disease (ARPKD) - congenital hepatic fibrosis (CHF), is characterized by the formation and expansion of fluid-filled cysts in the kidneys, enlargement of the kidneys and progressive fibrosis of both the kidney and the liver[1,2]. Caroli's disease, which manifests as cystic dilatation of the intrahepatic ducts, often accompanies ARPKD-CHF[3]. Afflicted children that survive past two years of age more often than not require renal and/or hepatic transplantation by age ten. The need for transplantation is driven as much by progressive organ dysfunction as by significant enlargement of the diseased organ(s) accompanied by severe pain[4].

Aberrant signaling by tyrosine kinases, including platelet-derived growth factor (PDGF) and vascular endothelial growth factor (VEGF) and their receptors (R), PDGFR and VEGFR/KDR, respectively, has been implicated in the formation and expansion of renal cysts. A PDGF-driven ciliopathy and/or overexpression of PDGF in the cyst lining and adjacent tubules are thought to, in part, drive renal cystic disease[5-7]. Cowley *et al*[8] posited that elevated and abnormal c-myc proto-oncogene expression drives ARPKD; c-myc expression is controlled by PDGF[9].

VEGF-driven angiogenesis is also thought to contribute to the growth of renal cysts, and inhibition of VEGFR/KDR signaling is associated with decreased tubule cell proliferation, decreased cystogenesis, and blunted renal enlargement[10,11]. Nevertheless, the role of VEGF in fibropolycystic disease is more controversial, with at least two reports suggesting that this growth factor might be associated with disease mitigation[12]. Aside from their roles in renal cyst formation and expansion, it is being recognized in ARPKD-CHF that aberrant PDGF and VEGF signaling are also associated with extracellular matrix deposition in the liver and kidney[13-15].

The PCK rat model is a well-established and well-characterized model that resembles human polycystic kidney and liver disease[16]. In the present study, we employed the PCK rat model to evaluate the therapeutic effects of ANG3070 on hepato-renal fibropolycystic disease. ANG3070 is an orally bioavailable, highly water-soluble, small molecule PDGFR and VEGFR/KDR inhibitor that binds

its target receptors with nanomolar affinity but exhibits limited interaction with other receptor tyrosine kinases as described by Panicker *et al*[17] and Narayan *et al*[18].

MATERIALS AND METHODS

Animal model

All studies relating to animals were approved by the Angion Biomedica animal use and care committee. Four week old male PCK/CrljCrl-Pkhd1^{pck}/Crl rats and age-matched male Sprague-Dawley (wild-type) rats were purchased from Charles River Labs (Wilmington, MA) and acclimatized for a week with a standard laboratory diet and water *ad libitum* at Angion prior to starting experiments. The PCK rat model includes ARPKD and autosomal dominant polycystic kidney disease (ADPKD). Many of the biochemical and morphological changes using these PCK rat models closely resemble human hepato-renal fibro polycystic disease[16]. We will use the best-characterized PCK rat model to establish therapeutic efficacy and the time window of our novel dual kinase inhibitor, ANG3070. PCK rats exhibit renal pathology starting from 4 wk of age with continuous progression of hepato-renal fibropolycystic disease with aging[16,17].

Sample size

Upon consultation with a biostatistician and based on formal power analysis, we expect a 30%-50% reduction in hepato-renal injury and pathology with ANG3070 treatment *vs* vehicle cohort, with a 30% standard deviation in each group and 80% power required to observe $P < 0.05$. Ten to 14 PCK rats were required for each group.

The total rats used in three separate experiments = approximately 18 wild type SD rats and 68 PCK rats. Some animals (PCK, $n = 2$; wild-type, $n = 4$) were sacrificed at 6 wk of age to confirm disease pathology. The PCK rats were then randomized to vehicle (water, $n = 14$) or ANG3070 (25 mg/kg, PO, BID; $n = 14$). Drug dose and dosing schedule was based on data (not shown) from previous studies in models of chronic kidney disease. At 10 wk of age (*i.e.*, after 4 wk of drug treatment), 24 h urine was collected, animals were anesthetized with isoflurane (2%), a midline incision was made and the left kidney was removed for analysis. Animals were then returned to their cages and allowed to recover. At 14 wk of age (*i.e.*, after 8 wk of drug dosing), 24 h urine was collected, animals were anesthetized, and the right kidney and liver were removed. For Western blot studies, 10 wk old male PCK rats were treated with vehicle or ANG3070 (25 mg/kg, PO, BID) for 7 d and sacrificed approximately 30 min after the last vehicle/drug administration. Kidneys were collected and stored in formalin and liquid N_2.

Cystic index

Cystic index (*i.e.*, the percentage of renal parenchyma occupied by cysts) was quantified using two independent blinded observers in hematoxylin and eosin (H and E) - stained kidney sections using digital planimetry (NIS Elements Viewer) as described previously[18]. The data from the two observers were averaged for each kidney.

Tissue and biomarker analysis

Body weight, kidney and liver masses were determined. Serum aspartate aminotransferase (AST), alanine aminotransferase (ALT), blood urea nitrogen (BUN) and serum creatinine (SCr) were measured by Northwell laboratory (New Hyde Park, NY). Proteinuria was measured using a modified Bradford and Lowry Bio-Rad protein assay and expressed as mg/24 h urine. Microalbuminuria (Abcam ELISA) was expressed as μg/24 h urine. Levels of neutrophil gelatinase-associated lipocalin (NGAL) (BioPorto Diagnostics, http://www.bioporto.com), cystatin C (R and D Systems, http://www.rndsystems.com), interleukin-18 (IL-18) (Biomedical Assay, http://www.biotechist.com) and kidney injury molecule-1 (KIM-1) (BioTrend, http://www.biotrend.com) were determined in urine samples using an enzyme-linked immunosorbent assay. Kidney and liver hydroxyproline, markers of tissue fibrosis, were measured from tissue homogenates[19] and expressed as μg/kidney or μg/liver.

Histopathology and immunohistochemistry

Formalin-fixed kidney and liver sections from PCK and/or wild-type rats were stained with Masson's trichrome or Picrosirius red to visualize collagen deposition in these tissues. The presence of multiple large and small cysts in the kidney and highly dilated irregular-shaped ducts in the liver, characteristic of this model of fibropolycystic kidney and liver disease, made it difficult to quantify fibrosis using histochemical stains. These stains therefore acted instead as a visual aid for the presence and location of matrix deposition in this model. Kidneys were also stained with anti-phospho PDGFR antibody (Antibody #3161, Cell Signaling) conjugated to horseradish peroxidase to visualize the presence and location of the activated receptor in this model of renal disease.

Western blot analysis

As described by Takikita-Suzuki *et al*[20], the frozen kidney tissue was homogenized on ice in buffer containing Tris-HCl (20 mmol/L; pH 7.5), ethylenediamine tetraacetic acid (1 mmol/L), NaCl (140 mmol/L), Nonidet P-40 (1%), aprotinin (50 μg/mL), NaF (50 mmol/L), sodium orthovanadate (1 mmol/L) and phenylmethyl sulfonyl fluoride (1 mmol/L). Homogenized tissue was centrifuged for 30 min at 15000 rpm at 4 °C. Supernatant was collected and protein concentrations were measured using the method of Bradford. After 12% sodium dodecyl sulfate-polyacrylamide gel electrophoresis, the protein was transferred to a nylon membrane (Amersham Pharmacia Biotech, Buckinghamshire, England, United Kingdom). Blocking was performed for 2 h in phosphate-buffered saline (PBS) solution containing 5% (w/v) skim milk,

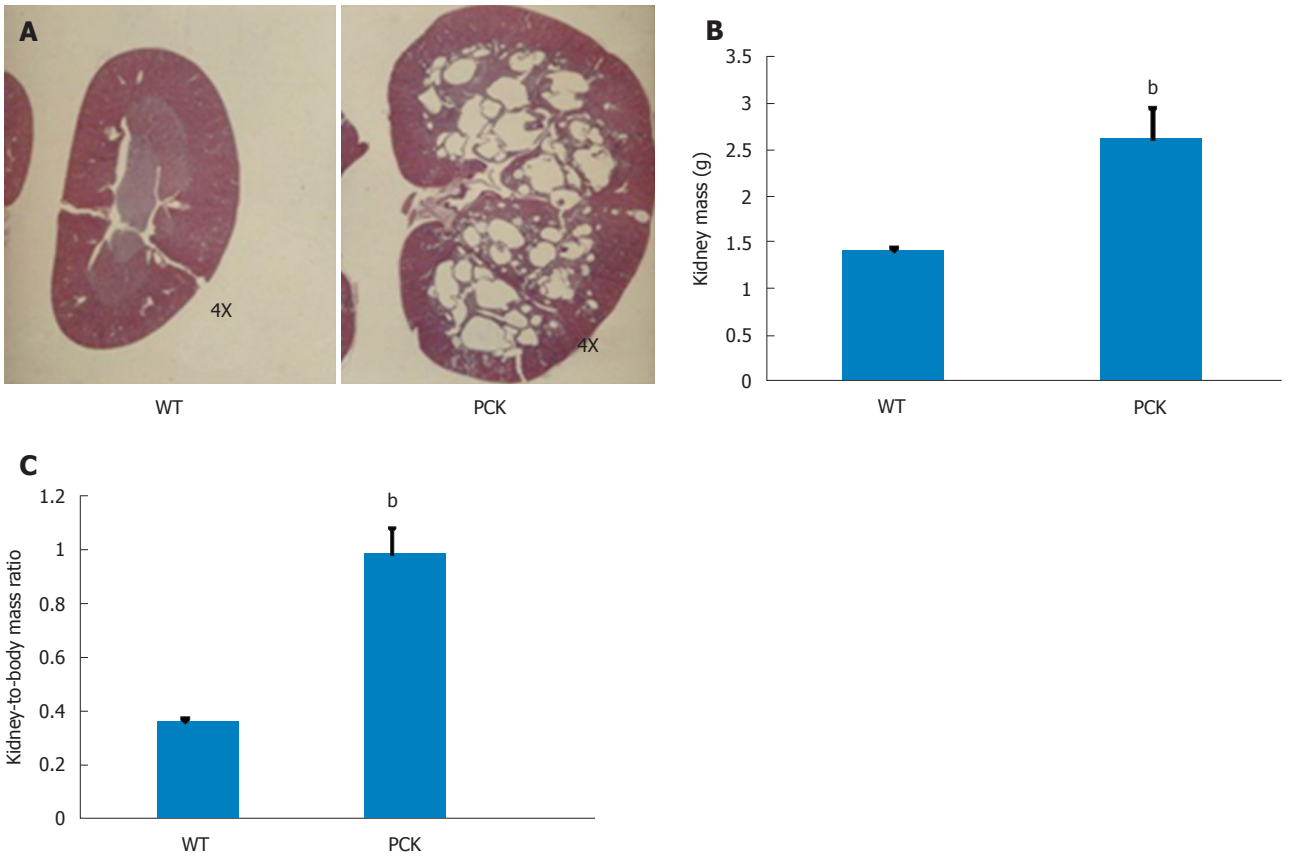

Figure 1 Renal characteristics in the PCK rat. A: Renal sagittal sections from 6 wk old wild-type (WT, Sprague-Dawley) and PCK rats showing an enlarged renal parenchyma and the medulla almost completely occupied with numerous cysts in the latter; B, C: At this time point, both kidney mass (B) and kidney-to-body mass ratio (C) were greater in the PCK rat ($^bP < 0.01$, *vs* WT).

followed with incubation with anti-α smooth muscle actin (α-SMA; Abcam) or anti-pPDGFRβ (Antibody #3161, Cell Signaling) antibodies, followed by an appropriate HRP-conjugated secondary antibody (Cell Signaling). Proteins were detected using an enhanced chemiluminescence kit (Amersham/GE Healthcare, United Kingdom). Densitometric analysis for pPDGFRβ was performed with normalization to GAPDH.

Statistical analysis

Data are presented as mean ± SD. Between-group effects were analyzed by one-way analysis of variance followed by Tukey's *post-hoc* test. A *P*-value < 0.05 is considered significant.

RESULTS

ANG3070 slows progressive kidney pathophysiology

Four-week treatment study: By approximately 6 wk of age, kidneys from PCK rats were enlarged and filled with numerous cysts (Figure 1). Both renal mass and renal-to-body mass ratio in PCK rats were significantly greater compared to the wild-type, age-matched cohort (Figure 1). By 10 wk of age, PCK rats (treated with vehicle, *i.e.*, 0.5 mL water, PO, BID) exhibited significant renomegaly compared to the wild-type cohort. Intervention with ANG3070 from weeks 6-10 was associated with a reduction in renal mass, renal-to-body mass ratio and renal cystic index (Figure 2). Compared to kidneys from wild-type animals, kidneys from PCK rats exhibited increased fibrosis, evidenced by increased tissue hydroxyproline content with ANG3070 treatment of the PCK rat associated with a reduction in renal hydroxyproline content (Figure 2). In addition to its effects on renal morphology, ANG3070 therapy was associated with the mitigation of kidney injury demonstrated by a reduction in 24-h urine NGAL and urine KIM-1 and amelioration of renal dysfunction, evidenced by reduced proteinuria and reduced albuminuria (Figure 2).

Eight-week treatment study: The effects of 8 wk of ANG3070 treatment were obvious in both kidneys and livers harvested from 14 wk old animals. At this time, the average kidney mass in the PCK rat (vehicle cohort) was several fold that of its wild-type counterpart and cystic index was approximately 30%. Nevertheless, a reduction in renal mass, renal-to-body mass ratio and cystic index was observed with drug treatment. At 14 wk of age, in addition to severe renal cyst formation, kidneys from PCK rats exhibited interstitial fibrosis evidenced by trichrome staining. The dominating presence of large cysts made analysis of the trichrome-stained area impractical, and

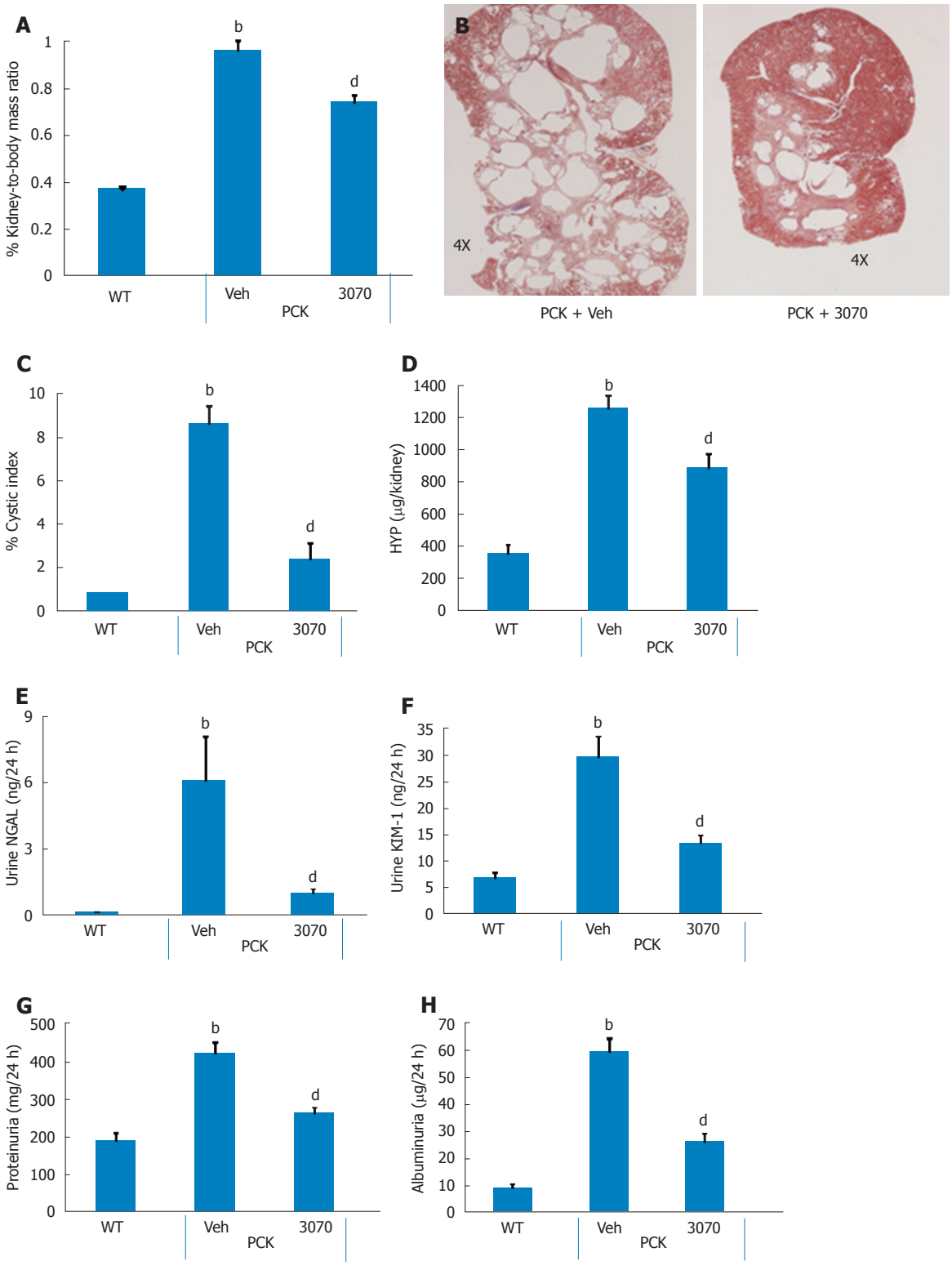

Figure 2 ANG3070 therapy attenuates renal mass, cystic index, renal injury, fibrosis and renal dysfunction. A, C: By approximately 10 wk of age, PCK rats [vehicle (Veh) cohort] had significantly larger renal mass and renal-to-body mass ratio (A) and increased cystic index (C) compared to the age-matched WT cohort ($^{b}P < 0.01$); B: Representative hematoxylin and eosin (HE)-stained renal sagittal sections (B) from PCK + Veh and a PCK + ANG3070 rats demonstrating cystic distribution across the renal parenchyma. Treatment of PCK rats with ANG3070 from weeks six to ten was associated with reduced kidney mass and kidney-to-body mass ratio (A) ($^{d}P < 0.01$, *vs* PCK + Veh); C: Treatment with ANG3070 reduced renal cystic index ($^{d}P < 0.01$, *vs* PCK + Veh); D: Total kidney hydroxproline (a marker of collagen) content was increased at week ten in the PCK (Veh) rat, treatment with ANG3070 was associated with a reduction in this marker of kidney fibrosis ($^{b}P < 0.01$, *vs* WT; $^{d}P < 0.01$, *vs* PCK + Veh); E, F: Compared to the WT cohort, PCK (Veh) rats exhibited renal injury evidenced by increased urine neutrophil gelatinase-associated lipocalin (NGAL) (E) and urine kidney injury molecule-1 (KIM-1) (F) ($^{b}P < 0.01$, *vs* WT). Treatment with ANG3070 was associated with a reduction in these urinary markers (E and F) of renal injury; G, H: Renal dysfunction, evidenced by elevated proteinuria (G) and albuminuria (H) was reduced with ANG3070 treatment ($^{d}P < 0.01$, *vs* PCK + Veh). HYP: Collagen marker.

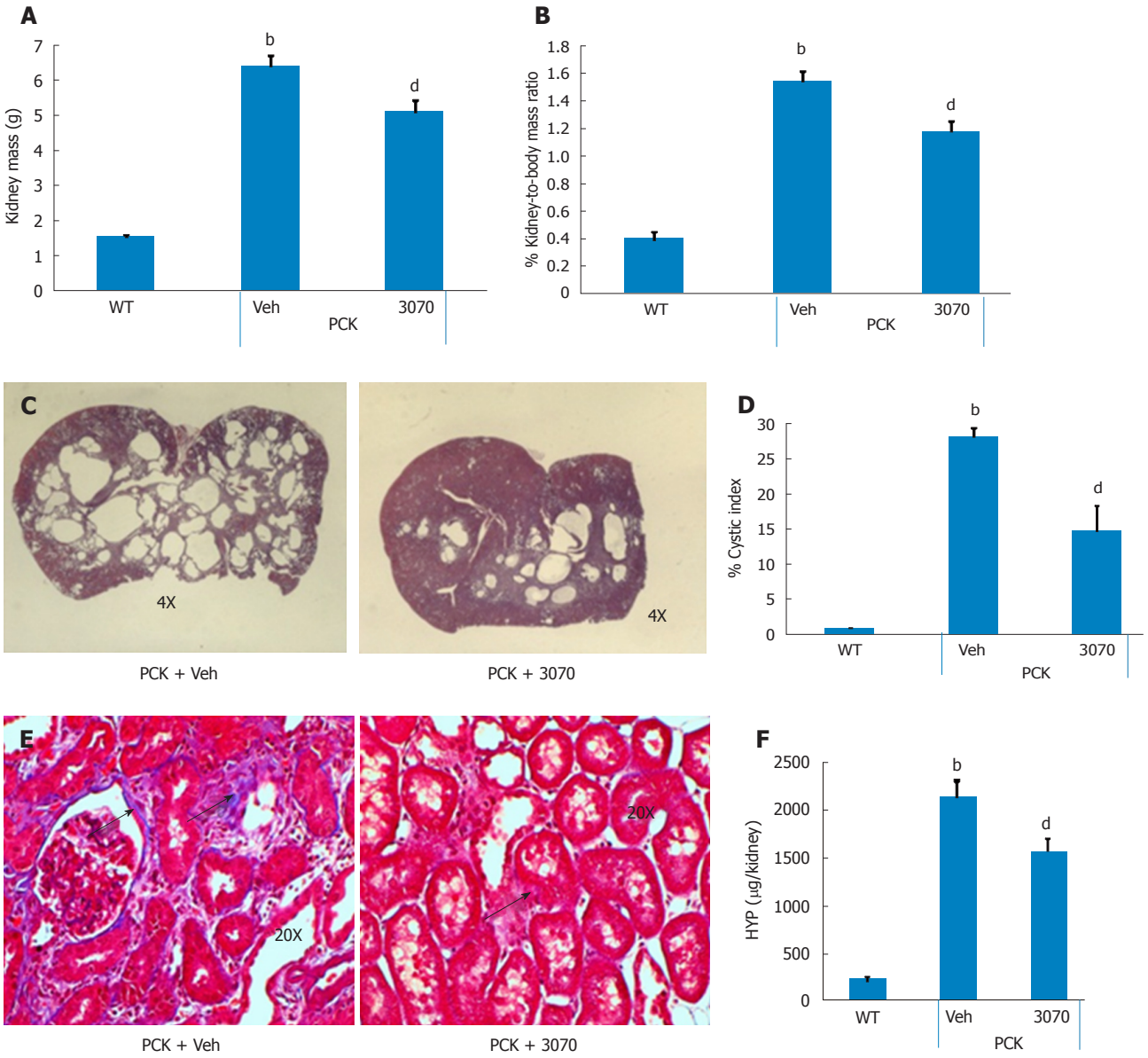

Figure 3 ANG3070 attenuates renal pathology and fibrosis in the PCK rat. A, B and D: By week 14, kidney mass (A), kidney-to-body mass ratio (B) and renal cystic index (D) were several-fold higher in PCK [vehicle (Veh)] rats compared to the WT cohort ($^{b}P < 0.01$, *vs* WT). ANG3070 therapy from weeks 6-14, mitigated renomegaly (A and B); C: Representative H and E-stained renal transverse sections from PCK + Veh and a PCK + ANG3070 rats demonstrating cystic distribution across the renal parenchyma at week 14; D: Treatment with ANG3070 reduced renal cystic index ($^{d}P < 0.01$, *vs* PCK + veh); E: Representative Masson's trichrome stained renal sections from PCK rats showing scarring within the renal interstitium (arrows) of PCK rats; F: Total kidney hydroxyproline (HYP-a marker of collagen) content was increased at week 14 in the PCK (Veh) rat ($^{b}P < 0.01$, *vs* WT). Treatment with ANG3070 was associated with a reduction in HYP, marker of kidney fibrosis ($^{d}P < 0.01$, *vs* PCK + Veh).

the extent of renal extracellular matrix deposition was therefore estimated biochemically in renal homogenates. Compared to the wild-type cohort, the PCK kidney (vehicle cohort) exhibited a marked increase in hydroxyproline content. Intervention with ANG3070 reduced renal fibrosis, evidenced by a decrease in total PCK kidney hydroxyproline content (Figure 3). Equally important, treatment with drug reduced renal injury, as evidenced by decreased 24-h urine - NGAL, KIM-1, cystatin C and IL-18 levels and attenuated key indices of renal dysfunction including proteinuria, albuminuria, BUN and SCr (Figure 4).

ANG3070 mitigates liver lesions: In addition to fibropolycystic kidney disease, PCK rats exhibit features of CHF and Caroli's disease, including hepatomegaly and ductal fibrosis with highly dilated intrahepatic ducts. Upon sacrifice (*i.e.,* approximately 14 wk of age), these characteristics of CHF and Caroli's disease were seen in PCK rats. Livers showed dilated intrahepatic ducts which were surrounded by matrix deposition, visible using H and E and Picrosirius red stains (Figure 5). Furthermore, frank hepatomegaly was evident in the PCK (vehicle) cohort. Although there was no increase in ALT (PCK *vs* wild-type, data not shown), AST was elevated. Treatment with

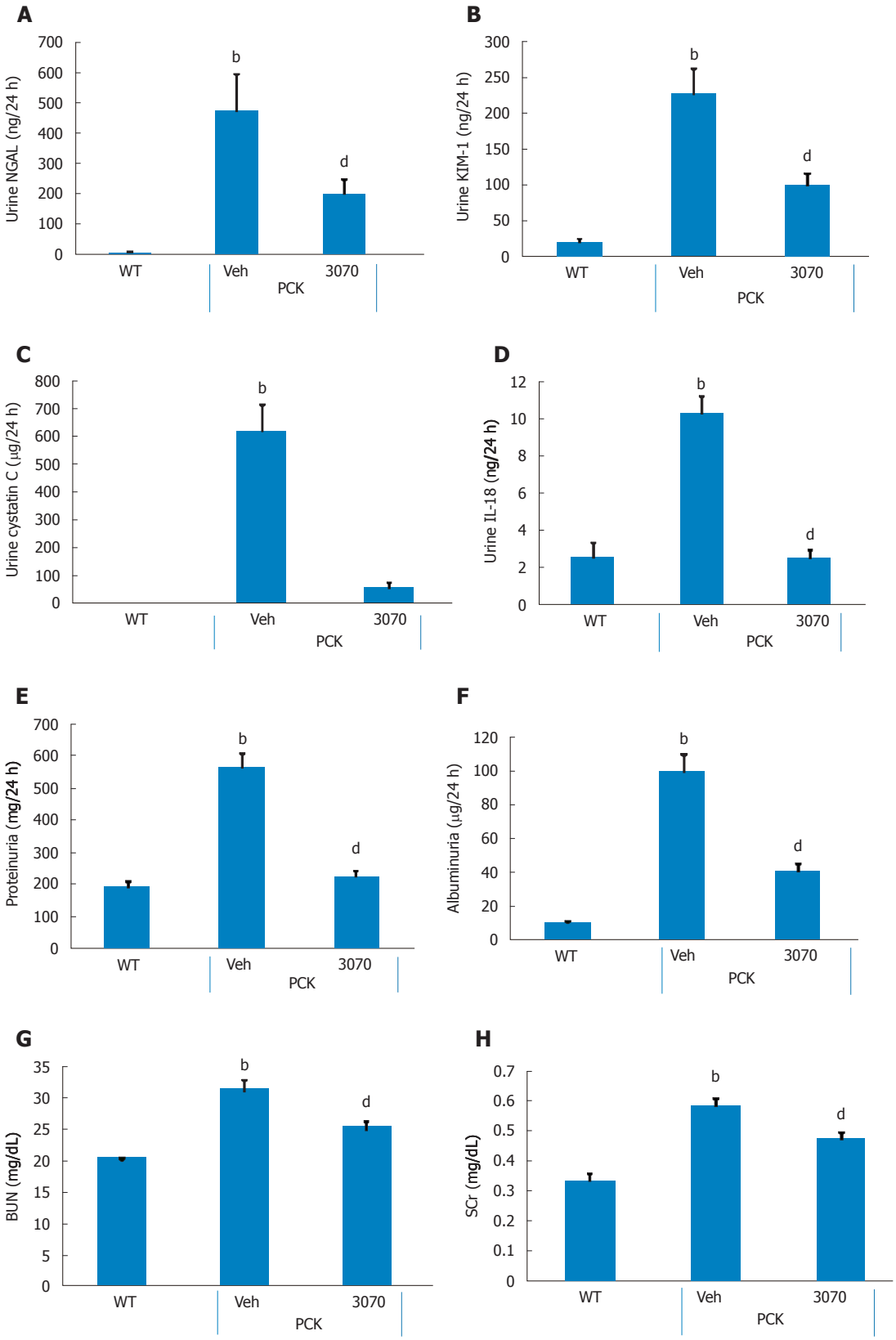

Figure 4 ANG3070 attenuates renal injury biomarkers and renal dysfunction. A-D: Compared to the WT cohort, at 14 wk of age, PCK [vehicle (Veh)] rats exhibited severe renal injury evidenced by increased urine - neutrophil gelatinase-associated lipocalin (NGAL) (A), kidney injury molecule-1 (KIM-1) (B), cystatin C (C) and interleukin-18 (IL-18) (D) ($^{b}P < 0.01$, *vs* WT). Treatment with ANG3070 was associated with a reduction in these urinary markers (A-D) of renal injury ($^{d}P < 0.01$, *vs* PCK + Veh); E-H: Renal dysfunction, evidenced by elevated proteinuria (E), albuminuria (F), blood urea nitrogen (BUN) (G) and serum creatinine (SCr) (H), was reduced with ANG3070 treatment ($^{b}P < 0.01$, *vs* WT; $^{d}P < 0.01$, *vs* PCK + Veh).

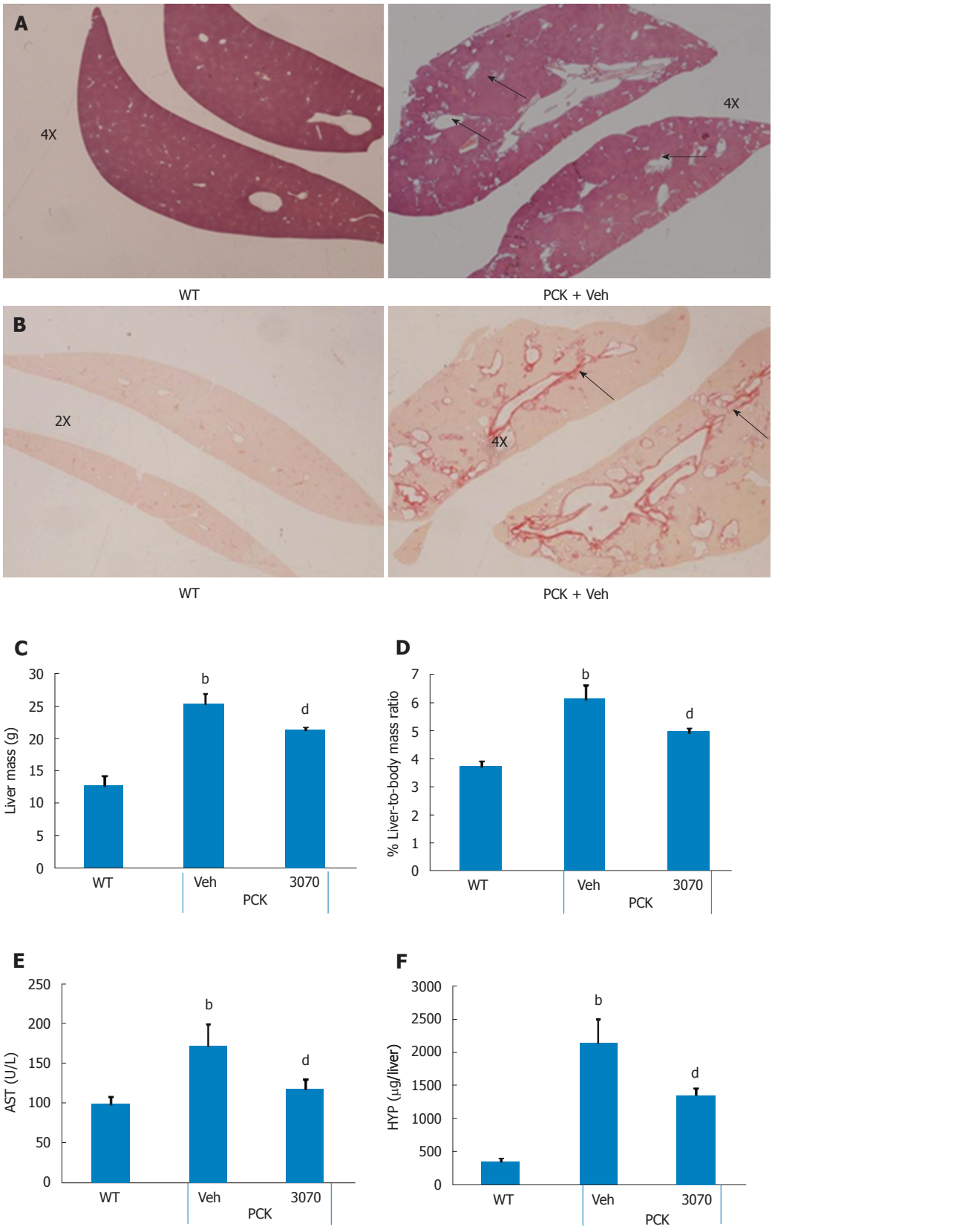

Figure 5 ANG3070 attenuates hepatic lesions, fibrosis and improves liver function in the PCK rat. A: Compared to the WT cohort, multiple, highly dilated bile ducts (arrows) are visible in H and E-stained PCK [vehicle (Veh)] livers by week 14; B: Representative Picrosirius red-stained liver showing ductal fibrosis (arrows) in the PCK (Veh) cohort; C-F: At sacrifice, PCK rats (Veh) exhibited increased liver mass (C), liver-to-body mass ratio (D) and aspartate aminotransferase (AST) (E) compared to the WT cohort. Total liver hydroxyproline content was also increased in the PCK rat (F). Treatment with ANG3070 was associated with a reduction in AST (E), hepatic lesions and fibrosis (HYP: Collagen marker) (A, B, C and F) ($^{b}P < 0.01$, *vs* WT; $^{d}P < 0.01$, *vs* PCK + Veh).

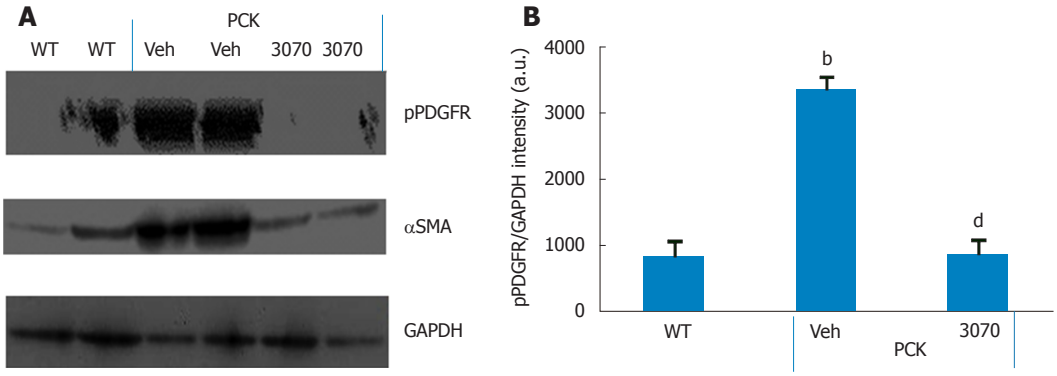

Figure 6 ANG3070 decreases phosphorylated platelet-derived growth factor receptor in the PCK rat kidney. A: Western blot analysis of kidney homogenates showed intense phosphorylated platelet-derived growth factor receptor (pPDGFR) levels in the PCK + vehicle (Veh) cohort compared to the WT and PCK + ANG3070 cohorts. A similar expression profile was seen with the fibrotic marker α smooth muscle actin (αSMA) in these kidneys. GAPDH expression is shown at the bottom; B: pPDGFR in renal homogenates from 10 wk old WT, PCK + Veh and PCK + ANG3070-treated animals was visualized with anti-PDGFR-α antibody and submitted to densitometric analysis with normalization to GAPDH. ANG3070 treatment was associated with a marked reduction in phosphorylated PDGFR levels ($^{b}P < 0.01$, *vs* WT; $^{d}P < 0.01$, *vs* PCK + Veh).

ANG3070 reduced liver mass, liver-to-body mass ratio, AST and total liver hydroxyproline content (Figure 5).

ANG3070 pharmacodynamics: It has been reported that the cystic milieu is enriched in growth factors such as PDGF[20]. The presence of multiple large and extensive cysts made immuno-histochemical quantification of pPDGFR impractical. Therefore, to determine whether the salutary effects of ANG3070 are associated with inhibition of this target, we evaluated the levels of pPDGFR together with the fibrotic marker α-SMA in renal homogenates from wild-type and vehicle- or ANG3070-treated PCK rats. As seen in Figure 6, compared to kidneys from wild-type animals, kidneys from the vehicle-treated PCK animals exhibited increased levels of both pPDGFR and α-SMA. In comparison to the PCK + Veh cohort, kidneys from the PCK + ANG3070 cohort exhibited decreased pPDGFR and α-SMA levels. Densitometric analysis of Western blots of renal homogenates from wild-type *vs* vehicle-treated PCK rats exhibited increased pPDGFR intensity, an effect that was reduced with ANG3070 treatment (Figure 6).

ANG3070 safety/toxicology profile: ANG3070 was efficacious and no potential toxic effects were observed in several rodent models. As detailed below, to date, there is no evidence of toxicity (liver or renal) in mice or rats dosed repeatedly over several weeks with ANG3070. In hundreds of mice and rats dosed several weeks with 150 mg/kg ANG3070 (PO, QD), there were no excursions in BUN (Veh 73 mg/dL; ANG3070 69 mg/dL) or SCr (veh 0.36 mg/dL; ANG3070 0.35 mg/dL) with ANG3070. In other rats dosed for 3 wk with ANG3070 (25 mg/kg, PO, BID × 3 wk), no excursions were seen in liver enzymes *vs* vehicle-dosed rats (ALT - veh: 92 IU; ANG3070: 61 IU; AST - Veh 158 IU; ANG3070 136 IU). There were no adverse events reported in 14 d toxicology studies in rats and dogs at nine-fold higher doses (450 mg/d) (data not shown) than the efficaceous dose of ANG3070 (50 mg/d) at which antifibrotic efficacy was observed in fibropolycystic kidney disease-CHF. These studies indicate that ANG3070 was safe and well-tolerated without any potential toxic effects. In PCK rats, treatment of ANG3070 for several weeks did not increase sCR, BUN, AST and ALT. In fact, sCR and AST were reduced with 3070 treatment. Overall ANG3070 was efficacious in decreasing kidney and liver fibrosis with no potential toxic effects in other organs.

DISCUSSION

We herein report that intervention with the orally bioavailable small molecule PAGFR and VEGFR dual kinase inhibitor ANG3070 ameliorates fibropolycystic disease progression in the PCK rat model of ARPKD-CHF. Intervention with this drug mitigated renomegaly, renal injury and renal dysfunction and fibrosis, effects associated with reduced renal PDGFR phosphorylation. Treatment with ANG3070 also reduced hepatic enlargement and fibrosis while improving liver function.

The formation and expansion of fluid-filled cysts drive kidney enlargement, with both an increasing cystic index and progressive extracellular matrix deposition driving functional insufficiency in fibropolycystic ARPKD-CHF[21,22]. A genetically-acquired and congenital disease, approximately 20-30% of affected patients succumb within the first 1-2 mo of life, with pulmonary insufficiency secondary to renal enlargement as the primary cause of death. For children making it past that stage, nephrectomy and dialysis or kidney transplant is often warranted by approximately ten years of age[23,24]. Intervention at this age is driven both by renal insufficiency and the need for a reduction in severe flank pain due to highly enlarged kidneys. The hepatic lesion in ARPKD-CHF is CHF resulting from a malformation of the ductal plate secondary biliary strictures and periportal

fibrosis, with the majority of patients also presenting with hepatomegaly[25,26]. Clinical studies in ARPKD-CHF reveal that a subset of patients progress to hepatocellular carcinoma[27]. Other than transplantation, there is no cure for ARPKD-CHF.

Mutations in the human *PKHD1* gene or mutations in *PKHD1* orthologs in rats and mice are required for development of ARPKD-CHF. However, experimental studies have identified that epithelial cells drive changes in the renal interstitium, with alterations in the cystic epithelia followed by changes in the interstitial fibroblasts and progressive accumulation of extracellular matrix. This ultimately leads to the development of renal fibrosis within that organ[28,29]. Furthermore, data from a number of studies suggest that growth factors, including PDGF and VEGF, are the intermediaries between the cystic and fibrotic components of progressive fibropolycystic disease[5,11]. A study[5] in the DBA/2FG-pcy mouse model of PKD suggests that increased expression of PDGF-A and PDGF-B chains may contribute to the progression of renal cystic lesions. Qin *et al*[30] reported impaired degradation of PDGFR in renal cells from PKD mice. In the ORPK murine model of PKD, responses to PDGF by fibroblasts, in which ciliary assembly is defective, are abnormal. In fact, Norman *et al*[31] identified a paracrine, PDGF-mediated regulatory loop between inner medullary collecting duct epithelial cells and medullary fibroblasts, highlighting the importance of tubular epithelial-interstitial fibroblast interactions in PKD. Compared to age-matched normal fibroblasts, PKD fibroblasts demonstrate an enhanced proliferative response to PDGF, synthesize more fibroblast growth factor, and elicit more rapid and persistent tyrosine phosphorylation of intracellular proteins. Consistent with these reports, pPDGFR signaling in our hands appeared to be increased in PCK rats compared to the wild-type cohort. PDGF activation was accompanied by upregulation of the fibrotic marker αSMA and matrix deposition in the renal interstitium. ANG3070 treatment decreased pPDGFR signaling and αSMA expression, indicating a decrease in fibrosis.

In the kidney, VEGF expression is most prominent in glomerular podocytes and in tubular epithelial cells, while VEGF receptors are mainly found on preglomerular, glomerular, and peritubular endothelial cells. Raina *et al*[32] reported that anti-VEGF therapy in the Han: SPRD rat, a model of ADPKD, was associated with an exaggerated cystic response of the proximal tubules and severe kidney injury. Huang *et al*[33] reported that VEGF therapy in the *Pkd1*$^{nl/nl}$ *mouse model of ADPKD was associated with robust benefits across a spectrum of endpoints, with far more modest benefits evident in the Cys1*$^{cpk/cpk}$ mouse, a model of ARPKD. On the other hand, it has been postulated that VEGF-driven angiogenesis drives cyst cells to grow, and may be responsible for increased vascular permeability and fluid secretion into the cysts. In fact, data from clinical trials point to a relationship between circulating VEGF and renal structural disease, including total renal volume, cyst volume and cyst number, and are indicative of a potential role for upregulated angiogenesis in early renal cyst progression[10-13]. Finally, Jiang *et al*[14] postulated that a pathogenic triumvirate, comprised by hyperproliferation of cyst wall growth, pericystic fibrosis, and inflammation, drives CHF/ARPKD progression.

ANG3070 is a proprietary, highly water-soluble, orally bioavailable potent inhibitor of PDGF and VEGF/KDR, which binds its targets with a K_d of approximately 5 nmol/L. In the PCK rat model of ARPKD-CHF, ANG3070 efficacy was observed across a spectrum of clinically-relevant endpoints, including a decrease in renomegaly, renal cystic index, renal injury markers, renal fibrosis and improvement in kidney function. Importantly, intervention with ANG3070, even after established renal disease at both 10 and 14 wk (a time when renal pathology is fairly advanced in the PCK rat), proved efficacious. Taken together, these data indicate that ANG3070 has therapeutic efficacy and slows a hallmark indicator of disease progression in ARPKD-CHF *via* cystic expansion of the kidney.

Another salient finding of this study was the effect of ANG3070 in mitigating renal injury in this model of ARPKD-CHF. Urinary markers of renal injury, including NGAL, KIM-1, cystatin C and IL-18, were increased in the PCK rat compared to wild-type controls. Previous studies have described the elevation of such markers in models of ARPKD-CHF. In fact, work by Nieto *et al*[34] indicates that BUN, SCr and 24-h urine IL-18 levels are biomarkers for increasing cystic index and increasing renal mass in the PCK rat. The fact that ANG3070 treatment was associated with a reduction of these biomarkers, including BUN, SCr and urine IL-18, not only suggests that this drug attenuates kidney injury but also suggests that it mitigates cystogenesis and renal expansion.

A pharmacodynamic exercise to confirm the mechanism of action of ANG3070 was undertaken in renal homogenates from the wild-type and PCK cohorts. Consistent with data from the aforementioned studies, PDGFR signaling was enhanced in the PCK rat kidney, evidenced by increased levels of pPDGFR. Administration of ANG3070 to the PCK rat reduced renal phosphorylated PDGFR levels, suggesting that the drug is indeed engaging its target and that the salutary effects of ANG3070 in the kidney are associated with inhibition of PDGFR signaling.

In addition to its effects on the kidney, ANG3070 exhibited activity against the hepatic lesions that accompany this disease. While hepatomegaly, elevated serum AST and increased hepatic collagen content were observed in the PCK rat at 14 wk of age, 8 wk treatment with ANG3070 resulted in significant amelioration of both liver pathology and liver dysfunction. This is an important finding, in that not only can hepatomegaly and hepatic fibrosis necessitate liver transplantation in

ARPKD-CHF patients, but also that a cytokine-driven feedback mechanism might exist between hepatic and renal lesions in this disease. Needless to say, there were some clear limitations to this study. Given the historical challenges associated with demonstrating a pharmacodynamic signature of VEGFR/KDR phosphorylation inhibition, we did not attempt to evaluate this signaling mechanism in the kidney or liver. Finally, the PCK rat is one model of ARPKD-CHF and it remains to be determined whether ANG3070 exerts similar effects in other models of this disease. In summary, intervention with ANG3070 favorably impacted both the renal and hepatic components in the PCK rat model of fibropolycystic disease. These data suggest that ANG3070 has the potential to slow ARPKD-CHF and may serve as a bridge toward hepato-renal transplantation in patients with fibropolycystic disease.

ARTICLE HIGHLIGHTS

Research background

In autosomal recessive polycystic kidney disease (ARPKD)-congenital hepatic fibrosis (CHF), a genetically acquired and congenital disease, mutations in the human *PKHD1* gene or mutations in *PKHD1* orthologs in rats and mice are required for the development of ARPKD-CHF. Nevertheless, experimental studies have identified that epithelial cells drive changes in the renal interstitium, with alterations made to the cystic epithelia followed by changes in the interstitial fibroblasts and progressive accumulation of extracellular matrix. This leads to the development of renal fibrosis within the kidney and/or liver. For children, nephrectomy and dialysis or kidney or liver transplant is often warranted by approximately ten years of age. Other than transplantation, there is no cure for ARPKD-CHF. We report that platelet-derived growth factor (PDGF) and vascular endothelial growth factor (VEGF) are the intermediaries between the cystic and fibrotic components of progressive fibropolycystic disease, and that a PDGFR + VEGFR dual inhibitor can be a novel therapeutic approach.

Research motivation

The development of new therapies that prevent the transition from cystogenesis to fibrosis or adenocarcinoma in advanced stages of ARPKD-CHF will have tremendous clinical potential and decrease the number of hepato-renal transplants in patients with ARPKD-CHF.

Research objectives

The main objectives of our studies were to evaluate a novel PDGFR and VEGFR dual kinase inhibitor, ANG3070, in a PKD-CHF model. These studies could lead to a novel therapeutic approach for fibropolycystic kidney disease.

Research methods

Renal pathology was confirmed in PCK rats at 6 wk compared to the age and gender-matched wild type SD rats. At 6 wk of age, PCK rats were then randomized to vehicle or ANG3070 for 4 wk. At 10 wk, 24 h urine and left kidneys were collected and rats were continued on treatments for 4 wk. At 14 wk, 24 h urine was collected, rats were sacrificed, and liver and right kidneys were collected for histological evaluation. For Western blot studies, PCK rats were treated with vehicle or ANG3070 for 7 d and sacrificed approximately 30 min after the last treatments.

Research results

A well-characterized PCK rat model was used to study fibropolycystic kidney disease. Compared to the wild-type cohort, the PCK kidney (Vehicle cohort) exhibited a marked increase in kidney and liver mass, hepato-renal cystic volume, hepato-renal fibrosis and hepato-renal injury biomarkers. Intervention with ANG3070 in PCK rats decreased kidney weight, reduced renal cystic volume and reduced total kidney hydroxyproline, thus indicating significantly reduced rental interstitial fibrosis compared to the PCK-Vehicle cohort. ANG3070 treatment also mitigated several markers of kidney injury, including urinary neutrophil gelatinase-associated lipocalin, kidney injury molecule-1, Cystatin C and interleukin-18 levels. This treatment also significantly attenuated key indices of renal dysfunction, including proteinuria, albuminuria and serum blood urea nitrogen and creatinine, and improved renal function compared to the PCK-Vehicle cohort. ANG3070 treatment also significantly decreased liver enlargement, hepatic lesions, decreased liver fibrosis and mitigated liver dysfunction compared to the PCK-Vehicle cohort. A dose-response study of ANG3070 needs to be evaluated to establish a minimum dose for maximal therapeutic efficacy in this PCK rat model.

Research conclusions

The development of new therapies that prevent the transition from cystogenesis to fibrosis or adenocarcinoma in advanced stages of ARPKD-CHF will have tremendous clinical potential. Studies indicate that PDGF and VEGF are the intermediaries between the cystic and fibrotic components of progressive fibropolycystic disease. We have identified and synthesized a novel small molecule PDGFR + VEGFR/KDR dual kinase inhibitor, ANG3070, using molecular modeling coupled with rational drug design, medicinal chemistry and structure activity relationship. We have evaluated ANG3070 therapeutic effects in a rat model of ARPKD-CHF and have proven it to be efficacious in mitigating kidney and liver injury biomarkers and decreasing hepatic and renal dysfunction. These studies could lead to the identification of a novel therapeutic approach in slowing fibropolycystic disease and decreasing the number of hepato-renal transplants in patients with ARPKD-CHF. These results suggest that ANG3070 has the potential in slowing disease, and may serve as a bridge toward hepato-renal transplantation in patients with fibropolycystic disease.

Research perspectives

The results of our studies suggest that ANG3070 has the potential therapeutic effect of slowing disease, and may serve as a bridge toward hepato-renal transplantation in patients with the fibropolycystic disease ARPKD-CHF.

REFERENCES

1 **Hartung EA**, Guay-Woodford LM. Autosomal recessive polycystic kidney disease: a hepatorenal fibrocystic disorder with pleiotropic effects. *Pediatrics* 2014; **134**: e833-e845 [PMID: 25113295 DOI: 10.1542/peds.2013-3646]

2 **Gunay-Aygun M**, Avner ED, Bacallao RL, Choyke PL, Flynn JT, Germino GG, Guay-Woodford L, Harris P, Heller T, Ingelfinger J, Kaskel F, Kleta R, LaRusso NF, Mohan P, Pazour GJ, Shneider BL, Torres VE, Wilson P, Zak C, Zhou J, Gahl WA. Autosomal recessive polycystic kidney disease and congenital hepatic fibrosis: summary statement of a first National Institutes of Health/Office of Rare Diseases conference. *J Pediatr* 2006; **149**: 159-164 [PMID: 16887426 DOI: 10.1016/j.jpeds.2006.03.014]

3 **Sung JM**, Huang JJ, Lin XZ, Ruaan MK, Lin CY, Chang TT, Shu HF, Chow NH. Caroli's disease and congenital hepatic fibrosis associated with polycystic kidney disease. A case presenting with acute focal bacterial nephritis. *Clin Nephrol* 1992; **38**: 324-328 [PMID: 1468163]

4 **ARPKD/CHF Alliance**. ARPKD/CHF Alliance Homepage. Available from: URL: http://www.arpkdchf.org

5 **Nakamura T**, Ebihara I, Nagaoka I, Tomino Y, Nagao S, Takahashi H, Koide H. Growth factor gene expression in kidney of murine polycystic kidney disease. *J Am Soc Nephrol* 1993; **3**: 1378-1386 [PMID: 8094982]

6 **Park JH**, Woo YM, Ko JY, Kim DY, Li X. Autosomal Dominant Polycystic Kidney Disease Induced by Ciliary Defects. **2015 [PMID:** 27512773]

7 **Torres VE**, Harris PC, Pirson Y. Autosomal dominant polycystic kidney disease. *Lancet* 2007; **369**: 1287-1301 [PMID: 17434405 DOI: 10.1016/S0140-6736(07)60601-1]

8 **Cowley BD Jr**, Smardo FL Jr, Grantham JJ, Calvet JP. Elevated c-myc protooncogene expression in autosomal recessive polycystic kidney disease. *Proc Natl Acad Sci USA* 1987; **84**: 8394-8398 [PMID: 3479800 DOI: 10.1073/pnas.84.23.8394]

9 **Frick KK**, Womer RB, Scher CD. Platelet-derived growth factor-induced c-myc RNA expression. Analysis of an inducible pathway independent of protein kinase C. *J Biol Chem* 1988; **263**: 2948-2952 [PMID: 2449430]

10 **Schrijvers BF**, Flyvbjerg A, De Vriese AS. The role of vascular endothelial growth factor (VEGF) in renal pathophysiology. *Kidney Int* 2004; **65**: 2003-2017 [PMID: 15149314 DOI: 10.1111/j.1523-1755.2004.00621.x]

11 **Bello-Reuss E**, Holubec K, Rajaraman S. Angiogenesis in autosomal-dominant polycystic kidney disease. *Kidney Int* 2001; **60**: 37-45 [PMID: 11422734 DOI: 10.1046/j.1523-1755.2001.00768.x]

12 **Spirli C**, Okolicsanyi S, Fiorotto R, Fabris L, Cadamuro M, Lecchi S, Tian X, Somlo S, Strazzabosco M. ERK1/2-dependent vascular endothelial growth factor signaling sustains cyst growth in polycystin-2 defective mice. *Gastroenterology* 2010; **138**: 360-371.e7 [PMID: 19766642 DOI: 10.1053/j.gastro.2009.09.005]

13 **Tao Y**, Kim J, Yin Y, Zafar I, Falk S, He Z, Faubel S, Schrier RW, Edelstein CL. VEGF receptor inhibition slows the progression of polycystic kidney disease. *Kidney Int* 2007; **72**: 1358-1366 [PMID: 17882148 DOI: 10.1038/sj.ki.5002550]

14 **Jiang L**, Fang P, Weemhoff JL, Apte U, Pritchard MT. Evidence for a "Pathogenic Triumvirate" in Congenital Hepatic Fibrosis in Autosomal Recessive Polycystic Kidney Disease. *Biomed Res Int* 2016; **2016**: 4918798 [PMID: 27891514 DOI: 10.1155/2016/4918798]

15 **Rajekar H**, Vasishta RK, Chawla YK, Dhiman RK. Noncirrhotic portal hypertension. *J Clin Exp Hepatol* 2011; **1**: 94-108 [PMID: 25755321 DOI: 10.1016/S0973-6883(11)60128-X]

16 **Lager DJ**, Qian Q, Bengal RJ, Ishibashi M, Torres VE. The pck rat: a new model that resembles human autosomal dominant polycystic kidney and liver disease. *Kidney Int* 2001; **59**: 126-136 [PMID: 11135065 DOI: 10.1046/j.1523-1755.2001.00473.x]

17 **Panicker B**, Mishra RK, Lim DS, Oehlen LJWM, Jung D. Antifibrotic Compounds and Uses Thereof. United States patent US9040555. 2012 Jan 26

18 **Narayan P**, Huang B, Prani PAKA, Paka L, Goldberg ID. Methods and uses of compounds for treating disease. United States patent US20150105380. 2013 Sep 23

19 **Samuel CS**. Determination of collagen content, concentration, and sub-types in kidney tissue. *Methods Mol Biol* 2009; **466**: 223-235 [PMID: 19148607 DOI: 10.1007/978-1-59745-352-3_16]

20 **Takikita-Suzuki M**, Haneda M, Sasahara M, Owada MK, Nakagawa T, Isono M, Takikita S, Koya D, Ogasawara K, Kikkawa R. Activation of Src kinase in platelet-derived growth factor-B-dependent tubular regeneration after acute ischemic renal injury. *Am J Pathol* 2003; **163**: 277-286 [PMID: 12819032 DOI: 10.1016/S0002-9440(10)63651-6]

21 **Al-Lawati TT**. Fibropolycystic disease of the liver and kidney in Oman. *Arab J Gastroenterol* 2013; **14**: 173-175 [PMID: 24433648 DOI: 10.1016/j.ajg.2013.11.004]

22 **Brancatelli G**, Federle MP, Vilgrain V, Vullierme MP, Marin D, Lagalla R. Fibropolycystic liver disease: CT and MR imaging findings. *Radiographics* 2005; **25**: 659-670 [PMID: 15888616 DOI: 10.1148/rg.253045114]

23 **Summerfield JA**, Nagafuchi Y, Sherlock S, Cadafalch J, Scheuer PJ. Hepatobiliary fibropolycystic diseases. A clinical and histological review of 51 patients. *J Hepatol* 1986; **2**: 141-156 [PMID: 3958471 DOI: 10.1016/S0168-8278(86)80073-3]

24 **Ko JS**, Yi NJ, Suh KS, Seo JK. Pediatric liver transplantation for fibropolycystic liver disease. *Pediatr Transplant* 2012; **16**: 195-200 [PMID: 22360404 DOI: 10.1111/j.1399-3046.2012.01661.x]

25 **Wilson PD**, Du J, Norman JT. Autocrine, endocrine and paracrine regulation of growth abnormalities in autosomal dominant polycystic kidney disease. *Eur J Cell Biol* 1993; **61**: 131-138 [PMID: 8223698]

26 **Schneider L**, Cammer M, Lehman J, Nielsen SK, Guerra CF, Veland IR, Stock C, Hoffmann EK, Yoder BK, Schwab A, Satir P, Christensen ST. Directional cell migration and chemotaxis in wound healing response to PDGF-AA are coordinated by the primary cilium in fibroblasts. *Cell Physiol Biochem* 2010; **25**: 279-292 [PMID: 20110689 DOI: 10.1159/000276562]

27 **Jain D**, Nayak NC, Saigal S. Hepatocellular carcinoma arising in association with von-Meyenburg's complexes: an incidental finding or precursor lesions? A clinicopatholigic study of 4 cases. *Ann Diagn Pathol* 2010; **14**: 317-320 [PMID: 20850692 DOI: 10.1016/j.anndiagpath.2010.04.003]

28 **Knecht A**, Fine LG, Kleinman KS, Rodemann HP, Müller GA, Woo DD, Norman JT. Fibroblasts of rabbit kidney in culture. Ⅱ. Paracrine stimulation of papillary fibroblasts by PDGF. *Am J Physiol* 1991; **261**: F292-F299 [PMID: 1652205 DOI: 10.1152/ajprenal.1991.261.2.F292]

29 **Sweeney WE Jr**, Avner ED. Molecular and cellular pathophysiology of autosomal recessive polycystic kidney disease (ARPKD). *Cell Tissue Res* 2006; **326**: 671-685 [PMID: 16767405 DOI: 10.1007/s00441-006-0226-0]

30 **Qin S**, Taglienti M, Nauli SM, Contrino L, Takakura A, Zhou J, Kreidberg JA. Failure to ubiquitinate c-Met leads to hyperactivation of mTOR signaling in a mouse model of autosomal dominant polycystic kidney disease. *J Clin Invest* 2010; **120**: 3617-3628 [PMID: 20852388 DOI: 10.1172/JCI41531]

31 **Norman JT**, Orphanides C, Garcia P, Fine LG. Hypoxia-induced changes in extracellular matrix metabolism in renal cells. *Exp Nephrol* 1999; **7**: 463-469 [PMID: 10559644 DOI: 10.1159/000020625]

32 **Raina S**, Honer M, Krämer SD, Liu Y, Wang X, Segerer S, Wüthrich RP, Serra AL. Anti-VEGF antibody treatment accelerates polycystic kidney disease. *Am J Physiol Renal Physiol* 2011; **301**: F773-F783 [PMID: 21677148 DOI: 10.1152/ajprenal.00058.2011]

33 **Huang JL**, Woolf AS, Kolatsi-Joannou M, Baluk P, Sandford RN, Peters DJ, McDonald DM, Price KL, Winyard PJ, Long DA. Vascular Endothelial Growth Factor C for Polycystic Kidney Diseases. *J Am Soc Nephrol* 2016; **27**: 69-77 [PMID: 26038530 DOI: 10.1681/ASN.2014090856]

34 **Nieto JA**, Yamin MA, Goldberg ID, Narayan P. An Empirical Biomarker-Based Calculator for Cystic Index in a Model of Autosomal Recessive Polycystic Kidney Disease-The Nieto-Narayan Formula. *PLoS One* 2016; **11**: e0163063 [PMID: 27695033 DOI: 10.1371/journal.pone.0163063]

P- Reviewer: El-Shabrawi MHF, Gheita TAA, Niu ZS, Tarantino G
S- Editor: Ji FF **L- Editor**: Filipodia **E- Editor**: Song H

World Journal of Nephrology

Submit a Manuscript: http://www.f6publishing.com

World J Nephrol 2018 September 7; 7(5): 108-116

DOI: 10.5527/wjn.v7.i5.108

ISSN 2220-6124 (online)

ORIGINAL ARTICLE

Basic Study

Unique interstitial miRNA signature drives fibrosis in a murine model of autosomal dominant polycystic kidney disease

Ameya Patil, William E Sweeney Jr, Cynthia G Pan, Ellis D Avner

Ameya Patil, William E Sweeney Jr, Cynthia G Pan, Ellis D Avner, Children's Research Institute; Children's' Hospital Health System of Wisconsin and the Medical College of Wisconsin, Milwaukee, WI 53226, United States

ORCID number: Ameya Patil (0000-0003-4666-2205); William E Sweeney Jr (0000-0001-9375-2348); Cynthia G Pan (0000-0002-1181-0901); Ellis D Avner (0000-0002-6734-1884).

Author contributions: Patil A, Sweeney Jr WE, Pan CG and Avner ED all equally contributed to the conception and design of this study, analysis, and interpretation of data; all authors drafted the article and made critical revisions related to the intellectual content of the manuscript, and approved the final version of the article to be published.

Supported by the Children's Research Institute, the Lillian Goldman Charitable Trust; Amy P Goldman Foundation; and Ellsworth Family and Children's Foundation of Children's' Hospital and Health System of Wisconsin.

Institutional animal care and use committee statement: All animal experiments are conducted in accordance with policies of the NIH Guide for the Care and Use of Laboratory Animals and the Institutional Animal Care and Use Committee (IACUC) of the Medical College of Wisconsin. The IACUC at the Medical College of Wisconsin is properly appointed according to PHS policy Ⅳ.A.3.a and is qualified through the experience and expertise of its members to oversee the Institution's animal care and use program. The Animal Welfare Assurance for the Medical College of Wisconsin is A3102-01. Specific protocols used in this study were approved by the Medical College of Wisconsin IACUC (approved protocols are AUA 4278 and AUA 4179).

Conflict-of-interest statement: The authors have no conflict of interest to declare. Conflict of Interest in Research statements is on file with the institution as per Medical College of Wisconsin policy #RS.GN.020.

Data sharing statement: Data sets and statistical methods are available upon request from the corresponding author

ARRIVE guidelines statement: The manuscript was revised according to the ARRIVE guidelines.

Open-Access: This article is an open-access article which was selected by an in-house editor and fully peer-reviewed by external reviewers. It is distributed in accordance with the Creative Commons Attribution Non Commercial (CC BY-NC 4.0) license, which permits others to distribute, remix, adapt, build upon this work non-commercially, and license their derivative works on different terms, provided the original work is properly cited and the use is non-commercial. See: http://creativecommons.org/licenses/by-nc/4.0/

Manuscript source: Unsolicited manuscript

Correspondence to: Ameya P Patil, MD, Assistant Professor, Department of Pediatrics, Medical College of Wisconsin, Children's Research Institute, Children's' Hospital Health System of Wisconsin, Children's Corporate Center, Suite 510, Mailstop CCC C510, 999 North 92nd Street, Milwaukee, WI 53226, United States. appatil@mcw.edu
Telephone: +1-414-9555773
Fax: +1-414-3377105

Received: April 21, 2018
Peer-review started: April 21, 2018
First decision: May 16, 2018
Revised: May 25, 2018
Accepted: July 31, 2018
Article in press: August 1, 2018
Published online: September 7, 2018

Abstract

AIM

To delineate changes in miRNA expression localized to the peri-cystic local microenvironment (PLM) in an orthologous mouse model of autosomal dominant

polycystic kidney disease (ADPKD) (*mcwPkd1*$^{(nl/nl)}$).

METHODS

We profiled miRNA expression in the whole kidney and laser captured microdissection (LCM) samples from PLM in *mcwPkd1*$^{(nl/nl)}$ kidneys with Qiagen miScript 384 HC miRNA PCR arrays. The three times points used are: (1) post-natal (PN) day 21, before the development of trichrome-positive areas; (2) PN28, the earliest sign of trichrome staining; and (3) PN42 following the development of progressive fibrosis. PN21 served as appropriate controls and as the reference time point for comparison of miRNA expression profiles.

RESULTS

LCM samples revealed three temporally upregulated miRNAs [2 to 2.75-fold at PN28 and 2.5 to 4-fold ($P \leqslant 0.05$) at PN42] and four temporally downregulated miRNAs [2 to 2.75 fold at PN28 and 2.75 to 5-fold ($P \leqslant 0.05$) at PN42]. Expression of twenty-six miRNAs showed no change until PN42 [six decreased (2.25 to 3.5-fold) ($P \leqslant 0.05$) and 20 increased (2 to 4-fold) ($P \leqslant 0.05$)]. Many critical miRNA changes seen in the LCM samples from PLM were not seen in the contralateral whole kidney.

CONCLUSION

Precise sampling with LCM identifies miRNA changes that occur with the initiation and progression of renal interstitial fibrosis (RIF). Identification of the target proteins regulated by these miRNAs will provide new insight into the process of fibrosis and identify unique therapeutic targets to prevent or slow the development and progression of RIF in ADPKD.

Key words: Inflammation; End-stage renal disease; Cysts; Autosomal dominant polycystic kidney disease; miRNA; Renal interstitial fibrosis

© The Author(s) 2018. Published by Baishideng Publishing Group Inc. All rights reserved.

Core tip: An essential and consistent histologic feature of progressive autosomal dominant polycystic kidney disease (ADPKD) is interstitial inflammation and fibrosis. This study investigated miRNA expression in local peri-cystic areas between cysts that become fibrotic as the disease progresses. This study identifies a critical limitation to whole organ transcriptomic approaches and demonstrates that laser capture microdissection (LCM) provides a means to overcome the dilutional factor of whole organ miRNA analysis. The precision of LCM provides a unique miRNA signature, which identifies novel molecular and therapeutic targets that initiate and drive interstitial fibrosis in ADPKD.

Patil A, Sweeney Jr WE, Pan CG, Avner ED. Unique interstitial miRNA signature drives fibrosis in a murine model of autosomal dominant polycystic kidney disease. *World J Nephrol* 2018; 7(5): 108-116 Available from: URL: http://www.wjgnet.com/2220-6124/full/v7/i5/108.htm DOI: http://dx.doi.org/10.5527/wjn.v7.i5.108

INTRODUCTION

Autosomal dominant polycystic kidney disease (ADPKD) is characterized by bilateral fluid-filled tubular cysts and progressive renal interstitial fibrosis (RIF). Renal function remains relatively normal until RIF reaches a tipping point, initiating a rapid decline of function leading to end-stage renal disease (ESRD).

miRNAs play key roles in diverse biological processes including cell division and death, intracellular signaling, cellular metabolism, immunity, and RIF. miRNAs are known to be involved in a variety of common human disorders including RIF[1, 2].

ADPKD is a common life-threatening renal disease that affects an estimated 12 million patients worldwide[3]. ADPKD is a heterogenetic disease with mutations in *PKD1* (MIM173910) (16p13.3) and *PKD2* (MIM173900) (4q22.1), which are responsible for approximately 80% and 15% cases respectively, with the remaining cases due to mutations at other rare loci[4].

Although ADPKD is a systemic disorder, it is characterized by the progressive development and growth of bilateral fluid-filled tubular cysts[5,6]. Renal cyst formation and expansion is followed by the development of RIF that ultimately leads to ESRD. Half of all ADPKD patients develop ESRD and require renal replacement therapy by their fifth decade[5,7].

Therapies currently in clinical trials focus on increased total kidney volume (TKV) as an indicator of disease severity, with decreased TKV reflecting the success of treatment[8-10]. However, an essential feature of the disease is interstitial inflammation and fibrosis[11-13]. Such interstitial changes lead to decreased TKV and strongly correlate with a decline in kidney function.

Renal fibrosis is the key determinant of the progression of all renal disease including ADPKD, irrespective of the original cause, and dictates the eventual outcome[11,13,14]. As cystic lesions enlarge, they compress both normal renal parenchyma and vascular elements between multiple cysts, creating a peri-cystic local microenvironment (PLM) that becomes fibrotic over time. The decline of renal function and the development of ESRD correlate with the progression of fibrosis in ADPKD[13,15,16]. Despite this link of ESRD to fibrosis, there is virtually no therapy specifically targeting fibrosis in ADPKD. This unmet clinical need calls for additional studies and a better understanding of the underlying mechanistic changes that lead to renal fibrosis.

Recent published studies have identified an essential role for miRNAs in the pathogenesis of both cyst formation and fibrosis in polycystic kidney disease[17-21]. miRNAs are short noncoding RNAs that regulate gene expression by reducing the translation of messenger RNAs[22-24]. miRNAs function in a diverse range of biological processes

and demonstrate spatial and temporal expression patterns[25]. MicroRNAs have been associated with many basic cellular processes as well as with a wide spectrum of diseases[1,24,25]. In the kidneys, miRNAs have been associated with renal development, homeostasis, and physiological functions[24,25]. Aberrant miRNA expression has been observed in mouse models of kidney fibrosis[18,20,26]. Notably, all previously published analysis has been performed in either whole kidney or cell culture models.

As cysts develop and enlarge, a local interstitial microenvironment is created between enlarging tubular cysts. This PLM is a complex milieu that integrates reciprocal signals from resident interstitial cells, infiltrating immune cells and proliferating cystic epithelial cells from enlarging tubular cysts. A complex interplay of many factors, including those driven by miRNA expression, occurs within the PLM. miRNAs play a role in determining the balance between pro-fibrotic and anti-fibrotic factors and how the dynamics of this balance drive the development of fibrosis[18,26]. In this study, we delineate changes in miRNA expression localized to the PLM in an orthologous mouse model of ADPKD (*mcwPkd1*$^{(nl/nl)}$). This model reliably demonstrates two phases of PKD: (1) the development and progressive enlargement of renal cysts, and (2) the development and progression of RIF, leading to loss of renal function. This model has a stable genetic background and permits both the investigation of pathogenic mechanisms and testing of potential therapeutic interventions. In the current study, we identify a unique PLM miRNA signature that drives fibrosis in this model.

MATERIALS AND METHODS

ADPKD mouse model (mcwPkd1$^{(nl/nl)}$*)*

The *mcwPkd1*$^{(nl/nl)}$ mice were generated as previously described[27]. Briefly, insertion of a neo-cassette into the Pkd1 allele (Pkd1nl) resulted in a cryptic splice site that allowed approximately 20% expression of a normal Pkd1 allele in homozygous *Pkd1*$^{(nl/nl)}$ mice[27]. In contrast to homozygous Pkd1 knockout mice, which are embryonically lethal, homozygous *mcwPkd1*$^{(nl/nl)}$ mice are viable, with bilaterally-enlarged polycystic kidneys by postnatal (PN) day 21, followed by the development and progression of RIF and ESRD between PN120 and PN150.

In the *mcwPkd1*$^{(nl/nl)}$ mouse, renal cystic lesions begin in utero, and TKV peaks by PN35. The initial appearance of light, wispy trichrome staining occurs in PLM at PN28.

All animal experiments were conducted in accordance with policies of the NIH Guide for the Care and Use of Laboratory Animals and the Institutional Animal Care and Use Committee (IACUC) of the Medical College of Wisconsin. The protocols used in this study were conducted under AUA 4379, which was approved by the Medical College of Wisconsin IACUC committee. The Animal Welfare Assurance for the Medical College of Wisconsin is A3102-01.

Sample preparation

Characterization of *mcwPkd1*$^{(nl/nl)}$ identified the time points of interest for this study. Triplicate samples from each of three time points were collected for analysis. These time points include: PN21, before evidence of collagen deposition with trichrome (controls); PN28, where trichrome-positive PLM was first evident; and PN42, when fibrosis was widespread. One kidney was placed directly in 10% formalin and paraffin-embedded (FFPE), and the contralateral kidney was flash frozen for RNA isolation.

Laser capture microdissection (LCM)

Serial 10 μm sections, at three different depths of the FFPE tissue, were floated onto PEN® membrane slides (Zeiss-415190-9081-000). A section from each of the three groups was stained lightly with McLethie's Trichrome stain for fibrosis. This stained section was used to guide LCM of its serial companion section. LCM of PN21 was accomplished by taking areas between multiple cysts due to the absence of trichrome-positive areas. The PN21 pre-fibrotic cystic kidney was used as the appropriate control, because aged-matched wildtype kidney is devoid of adequate interstitial areas for comparitive analysis (Figure 1).

RNA extraction

After harvesting 300000 um² of PLM, total (miRNA and mRNA) RNA was extracted with Qiagen's miRNeasy FFPE kit (Qiagen #217504) according to the manufacturer's instructions. The isolated total RNA was converted to cDNA using the miScript Ⅱ RT Kit (Qiagen #218161), according to the manufacturer's instructions, and was subsequently amplified using the miScript PreAMP PCR kit (Qiagen #331452). The amplified cDNA was used for reverse transcription PCR using the miRNome miScript miRNA PCR Array (Qiagen #331222) to assess changes in miRNA expression over time. miRNA profiling of contralateral whole kidney samples was similarly performed as described above.

Quality control

The quality of the samples was assessed by determining the 260/280 ratios and RNA integrity numbers (RIN) using the Agilent 2100 bioanalyzer and RNA 6000 Pico kits, respectively. RNA samples with a 260/280 ratio > 1.6 yielded an RIN between 7 and 9. RINs > 7 passed the internal RNA quality control test of the Qiagen miRNA plates. Samples with a 260/280 ratio > 1.6 were analyzed immediately and had to pass the internal controls of the plates to be included in our analysis. The RIN of the samples was periodically obtained. In all cases where the 260/280 ratio exceeded 1.6, RIN values

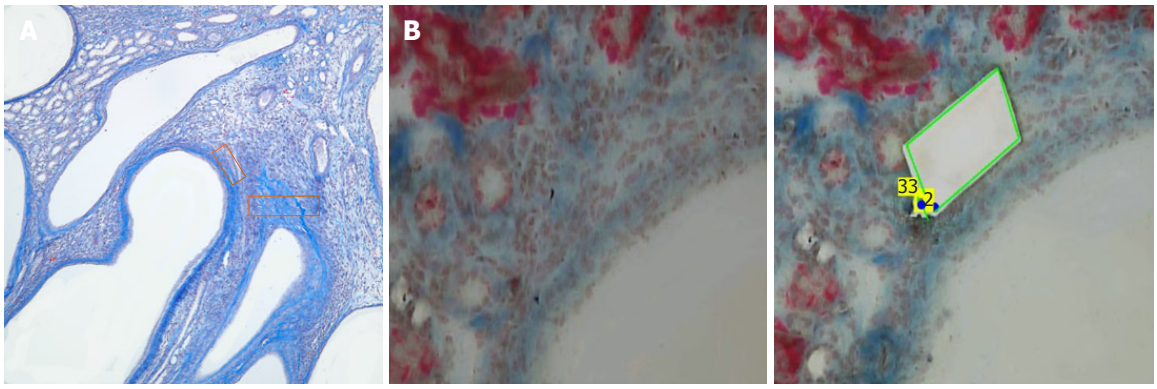

Trichrome stained section of ADPKD kidney | Pre-LCM | Post-LCM

Figure 1 Laser capture microdissection of the peri-cystic local microenvironment. A: Trichrome-stained section of a dominant polycystic kidney diseased (ADPKD) kidney with representative laser capture microdissection (LCM) areas marked by red rectangles; B: Trichrome-stained section of an ADPKD kidney before and after LCM.

exceeding 7.0 were obtained and passed the internal controls of the Qiagen plates.

Trichrome staining

Slides were deparaffinized in xylene, then rehydrated in 95% ETOH. Slides were then stained with McLethie's Trichrome (Newcomer Supply #9177), according to the manufacturer's instructions.

Statistical analysis

A total of three animals were included at each time point (PN21, PN28 and PN42) for both the LCM and whole kidney groups. Data were normalized for miRNA expression to stably-expressed housekeeping genes (*SNORD68* and *SNORD96A*) at each time point. Whole kidney miRNAs from contralateral kidneys were similarly examined at PN21, PN28 and PN42.

Average CT values and the standard deviations for the miRNAs expressed were examined. A sample size of $n = 3$, sufficient for appropriate statistical analysis, was selected. Data was analyzed using the Qiagen® online portal and GraphPad® Instat 3. Data are expressed as a change in expression for a particular miRNA (fold-regulation) at PN28 and PN42 compared to PN21 for both the PLM region and whole kidney. Only changes +/- 2-fold are included in the analysis. $P \leqslant 0.05$ was considered significant.

TargetScan and miRDB websites were used to determine targets for the miRNAs.

RESULTS

More than 900 miRNAs were examined in the laser captured PLM at the three different time points (PN21, PN28, PN42). miRNA expression in PLM at two different time points (PN28 and PN42) was compared with PN21 in order to: (1) provide a relative change in the expression of miRNAs during the onset of fibrosis; and (2) reflect local micro-environmental changes with disease progression.

Whole kidney miRNA changes compared with PLM miRNA changes

Whole kidney miRNA expression was compared to the miRNA expression profiles obtained from laser captured PLM samples at PN28 and PN42, with PN21 as a control (Figure 2). The heat maps show major differences in the expression levels of key miRNAs between the whole kidney and PLM areas (Figure 2).

PLM miRNA changes with onset of fibrosis at PN28

The mechanism(s) by which miRNAs represses translation allows us to make certain predictions. An increase in miRNA expression would likely lead to a reduction in the level of the target protein, and a decrease in miRNA expression would yield an increase in the target protein.

In Figure 3A, there are three miRNAs that show temporal increase in expression at PN28 and PN42. miR-667-3p, miR-3074-5p and miR-7b-3p are upregulated 2 to 2.75-fold at PN28, and are further upregulated to 2.5 to 4-fold and reach statistical significance at PN42.

In Figure 3B, a similar comparison made for sequentially downregulating miRNAs shows that a total of four miRNAs that are downregulated at PN28 continue to further decrease expression at PN42. miR-378a-3p, miR-30e-5p, miR-30a-5p and miR-344f-5p are downregulated 2 to 2.75-fold at PN28, and are further reduced 2.75 to 5-fold and reach statistical significance at PN42.

PLM miRNA changes with progressive fibrosis at PN42

Figure 4 show the results of PLM miRNA changes at PN42, which represents a stage of progressive fibrosis.

miRNAs with decreased expression > 2-fold at PN42 are shown in Figure 4A. miR-484, miR-455-3p, miR-130a-3p, miR-93-5p, miR-106-5p and miRN-677-3p are significantly downregulated in the range of 2.25 to 3.5-fold. miR-106-5p showed the largest decrease at 3.5-fold.

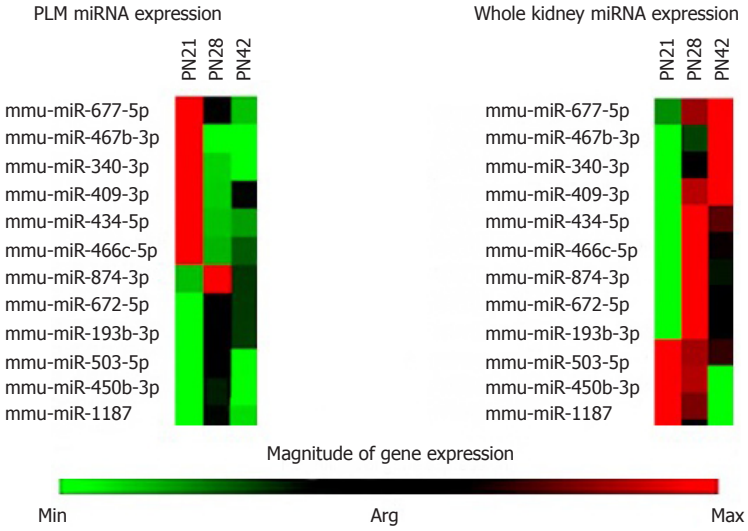

Figure 2 Heat map comparing miRNA expression. Heat map showing comparative expression of a set of miRNAs at three different post-natal (PN) time points (PN21, PN28 and PN42) for peri-cystic local microenvironmental regions and whole kidney samples (green represents downregulated miRNA expression, whereas red represents upregulated miRNA expression).

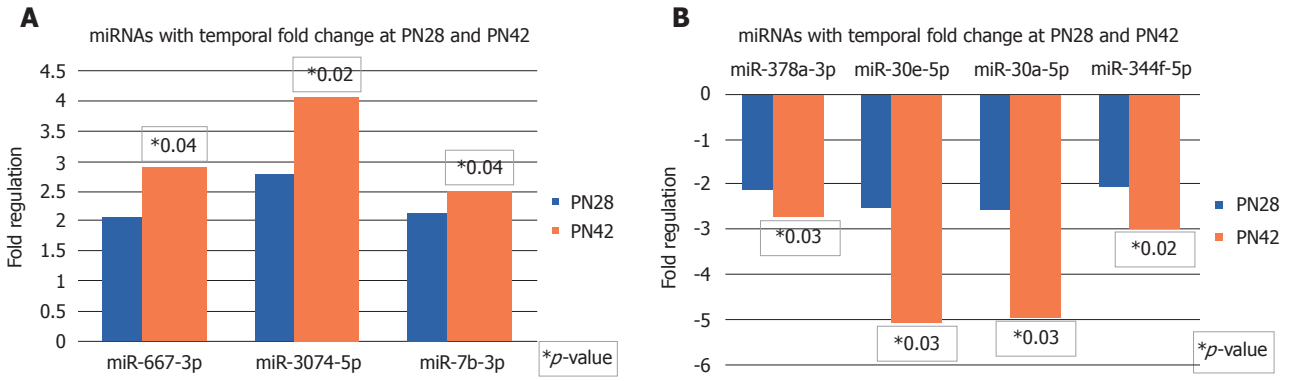

Figure 3 miRNA expression profiles. Expression profiles of a set of miRNAs at PN28 and PN42 that are temporally upregulated (A) and downregulated (B) when compared with PN21 in peri-cystic local microenvironmental regions.

miRNAs with increased expression >2-fold at PN42 are shown in Figure 4B. miR-409-3p, miR-762, miR-298-5p, miR-149-5p, miR-186-5p, miR-125a-3p, mIR-331-3p, miR-155-5p, miR-329-3p, miR-186-5p, miR-376c-3p, miR-665-3p, miR-383-5p, miR-107-3p, miR-542-3p, miR-672-5p, miR-32-5p, miR-96-5p, miR-503-5p and miR-466d-3p are significantly upregulated (2 to 4-fold).

DISCUSSION

In ADPKD, despite massive increases in kidney size, loss of renal function and progression to ESRD is largely dependent upon the development of renal fibrosis[11]. In the *mcwPkd1*$^{(nlnl)}$ mouse, we discovered that fibrosis started in discreet areas between multiple cysts at PN28, evidenced by light wispy trichrome-positive staining in sporadic areas between multiple cysts. Similar areas between multiple cysts were evident in PN21 kidneys, but they never showed positive trichrome staining. By PN42, trichrome staining revealed a spread of the fibrosis outward from PLM. This suggested to us that we may be able to identify critical elements necessary for the initiation and progression of fibrosis by using LCM to capture and analyze changes in PLM areas at the specific time-points noted. PN21 PLM areas provided appropriate controls, as they are devoid of fibrosis. Wild-type tissue was not an appropriate control in this experiment because it has minimal interstitial tissue that can be targeted for LCM. The risk of contaminating the wild-type LCM samples with epithelial tissue is unacceptably high.

Many previous studies have examined miRNA expression in whole kidneys to study progressive renal diseases[18,21,28-30]. However, a critical limitation to transcriptomic approaches of whole kidney is the kidney's cellular complexity: arrays from whole kidney reflect the averaged= expression of 26 or more different cell types[31-33]. This limitation is exacerbated in the presence of inflammatory cells in diseased kidneys.

The most striking result of these studies was the difference in miRNA profiles from PLM and whole kidney as shown in cluster heat maps (Figure 2). The expression of miRNAs in PLM is very different when compared to

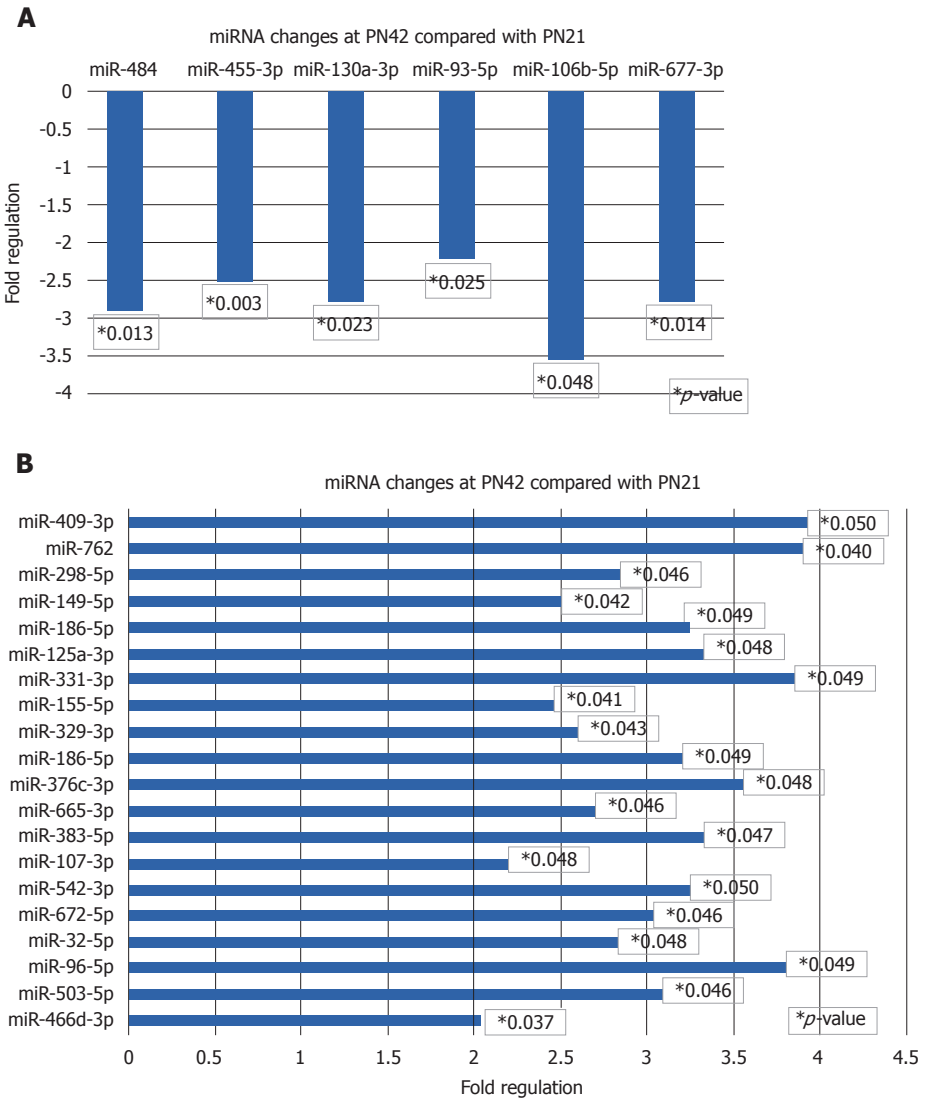

Figure 4 miRNA expression profiles. Expression profiles of a set of miRNAs with significantly decreased (A) and increased (B) expression at PN42 in peri-cystic local microenvironmental regions compared with PN21.

whole kidney expression. These findings likely reflect a dilution of important local changes in miRNAs when whole kidney comparisons are made. The implication of this is clear. Relying on whole kidney analysis may lead one to make errors in interpreting miRNA data.

The key miRNA changes noted in PLM, interestingly, are involved in or have predicted targets that play a role in the pathogenesis of either fibrosis, PKD or are unique. miRNAs with decreased expression at PN28 and PN42 (Figure 3B) have predicted targets (listed in brackets) as follows: miR-30a-5p and miR-30e-5p (Socs6, Timp2, Rock2, Bcl6, Col9a3, Col13a1, Smad1, Irf4) and miR-378a-3p (Mapk). Timp2 inhibits extracellular matrix proteolysis in multiple tissues, thus promoting fibrosis. Rock2, Irf4 and BCL6 have known roles in macrophage polarization, which plays an important role in the process of both inflammation and fibrosis. Mapk is an important mediator in the pathogenesis of PKD[34]. The expression of these miRNAs sequentially decreases at PN28 and PN42, which correlates with worsening PLM fibrosis.

Moreover, there are six additional interesting miRNAs that have decreased expression in PN42 PLM (Figure 4). These miRNAs with their targets are as follows: miR-484 (Tgfβr3, Fgf1), miR-455-3p (HB-EGF), miR-130a-3p (Tgfβ2, Tgfβr1, Tnf, Wnt1, Pparγ), miR-677-5p (Col15a1), miR-106b-5p and miR-93-5p (Fgf4, Vegfa, Stat3, Mapk4, Mapk9, Hif1α, Pparα, Col4a3, Col4a4). Tgfβ and Tgfβr are integral to the processing of fibrosis, but are involved in late stages of progressive fibrosis[35]. HB-EGF is a member of the EGF family of proteins and is produced by monocytes and macrophages[36,37]. Recently, high urinary levels of HB-EGF are discovered in the urine of patients with severe PKD[36-38]. Stat3 plays an important role in the pathogenesis of PKD[39,40]. Hif1 has roles in angiogenesis, fibrosis, and is closely tied to local hypoxia[35], which may be the direct result of expanding cystic lesions.

Furthermore, PLM miRNAs with increased expression at PN42 are shown in Figure 4A and their predicted targets are as follows: miR-466d-3p (Smad7), miR-

542-3p (Bmp7), miR-96-5p (βRaf, Nox4), miR-186-5p and miR-329-3p (Usf2) miR-762 (Cx3cl1), miR-155-5p (Socs1, Csf1r), and miR-331-3p (Mmp13). Smad7 inhibits TGF-β signaling by preventing formation of Smad2/Smad4 complexes[35,41]. BMP7 reduces extracellular matrix formation and hence fibrosis[35]. With increased expression of miRNAs, the targets Smad 7 and BMP7 are expected to decrease and hence promote fibrosis. Along with these miRNAs, there are many other novel miRNAs that should be considered for further investigation.

Realizing that all forms of fibrosis eventually involve the TGF-β pathway, we anticipated we would see a few unique differences in miRNA profiles at PN28, the initiation point of fibrosis. We were surprised by the degree of difference and the fact that some were maintained at least through PN42, as seen in Figure 3. Some changes may reflect differences in canonical and non-canonical TGF-β signaling cascades. However, the majority of differences are not likely due to different TGF-β pathways but rather due to differences in methodology. Other changes may reflect key differences in methodology utilized in this study.

A dilution effect created by using an organ with 26 different cell types must be considered when examining miRNAs in whole kidney samples. This has huge implications in the pursuit of therapeutic interventions. The heat map in Figure 2 demonstrates that while the identification of miRNAs that change may be the same with both techniques, the direction of change for some miRNAs goes in opposite directions. This could lead to a situation where a therapy based on whole organ analysis could exacerbate the disease. More importantly, LCM-obtained tissue is expected to represent the local pathology of interest that is being studied.

Fibrosis seen in this ADPKD model is initially localized to discrete areas between multiple cysts, which then expand with the progression of disease. The PLM in which fibrosis occurs undergoes multiple molecular and cellular changes with disease progression. The PLM areas isolated by LCM include locally proliferating cells that likely have key roles in the process of fibrosis. The changes preceding early fibrosis in the PLM of ADPKD kidneys act as a trigger factor that then stimulate cells locally to lay down collagenous extracellular matrix, which causes fibrosis. The isolation of these areas with LCM, as well as examining them at various stages before and after the onset of fibrosis, offers unique insight into this dynamic microenvironment.

Further work is required to identify the phenotypes of these cells and their specific roles. A large number of cells in PLM tissue from ADPKD are phenotypically identified as macrophages. Their role in fibrosis has been well studied and reported[42]. Some or many of these PLM miRNA changes may be directly or indirectly related to macrophage changes that then drive the process of fibrosis. miRNAs are known to modulate macrophage activation and miRNAs are shown to be induced by hypoxia/ischemia. With cyst expansion and compression of parenchyma between these expanding cysts, local hypoxia and ischemic changes can be expected early in the disease course of ADPKD. Whether such hypoxic/ischemic changes drive the early changes in the cellular make-up of the peri-cystic interstitium and drive PLM miRNA changes remain to be investigated.

In conclusions, this study identifies a unique interstitial miRNA signature that drives fibrosis in the new *mcwPkd1*$^{nl/nl}$ model of ADPKD. Such changes in miRNA profiles in ADPKD PLM obtained by LCM provide unique insight into signaling in local areas where fibrosis begins. These PLM miRNA changes are not seen in whole kidney miRNA analysis. These PLM miRNAs have unique predicted targets, and some have established roles in hypoxia, proliferation, angiogenesis and fibrosis. Many of the LCM miRNAs identified are unique and represent new candidates for further study. This approach identifies novel future molecular and therapeutic targets. Further cell-specific miRNA expression studies will provide valuable information in further identifying potential therapeutic targets of fibrosis in ADPKD.

ARTICLE HIGHLIGHTS

Research background

Autosomal dominant polycystic kidney disease (ADPKD) is the most common genetic renal condition, with an incidence of 1 in 500 to 1000 individuals. ADPKD affects approximately 750000 people in the United States and 12.5 million people worldwide. Nearly 50% of ADPKD patients will develop kidney failure that requires dialysis or transplantation. To date, clinical trials targeting cyst growth (epithelial proliferation) have been largely ineffective in improving or slowing the decline in renal function, despite reducing epithelial proliferation and total kidney volume (TKV). Tolvaptan, the most promising therapy to date, has an estimated cost of $744100 per year per quality-adjusted life-year gained compared with standard care.

Research motivation

In ADPKD, as fluid-filled cysts develop and enlarge, a peri-cystic local microenvironment (PLM) is created between the cysts, which become fibrotic over time. TKV decreases with such fibrotic changes and has a strong correlation with loss of renal function. Despite this connection between fibrosis and end-stage renal disease (ESRD), there is no experimental or FDA-approved therapy that specifically targets fibrosis in ADPKD.

Research objectives

To investigate miRNA expression in PLM between cysts that become fibrotic as disease progresses.

Research methods

We employed LCM to analyze the miRNA profile of PLM at PN21, prior to any morphometric sign of fibrosis (trichrome stain), and at two time points of increasing degrees of fibrotic severity at PN28 (initiation) and PN42 (progression). These results were compared to age-matched expression profiles of whole kidney analysis of the miRNA expression profile.

Research results

The most striking result of these studies was the difference in miRNA profiles from PLM and whole kidney, as shown in cluster heat maps. The expression of miRNAs in the PLM was significantly distinct when compared to whole kidney expression.

Research conclusions

Relying on whole kidney analysis may lead one to pursue not only the wrong

miRNA, but may also lead to targeting a miRNA or protein that exacerbates the disease process you are trying to ameliorate. Therefore, published data that relies upon whole kidney transcriptomic analysis should be viewed with careful skepticism. Identification of the molecular and cellular changes in the PLM will lead to new therapeutic targets, with the potential to prevent the initiation or slow the progression of fibrosis.

Research perspectives

This study presents a unique approach to identify novel molecular and therapeutic targets that initiate and drive interstitial fibrosis in ADPKD. The use of therapies targeting fibrosis alone or in combination with therapies targeting epithelial proliferation will dramatically improve the quality of life of ADPKD patients by extending the time to ESRD.

ACKNOWLEDGMENTS

The authors thank Nick Kampa and Emma Schwasinger for their dedication and excellent technical skills that made these experiments possible. The authors also thank Dr. Dorien Peters for providing *Pkd1*$^{(nl/nl)}$ mice to develop the unique *mcwPkd1*$^{(nl/nl)}$ model as described.

REFERENCES

1 **Li Y**, Kowdley KV. MicroRNAs in common human diseases. *Genomics Proteomics Bioinformatics* 2012; **10**: 246-253 [PMID: 23200134 DOI: 10.1016/j.gpb.2012.07.005]

2 **Bae K**, Park B, Sun H, Wang J, Tao C, Chapman AB, Torres VE, Grantham JJ, Mrug M, Bennett WM, Flessner MF, Landsittel DP, Bae KT; Consortium for Radiologic Imaging Studies of Polycystic Kidney Disease (CRISP). Segmentation of individual renal cysts from MR images in patients with autosomal dominant polycystic kidney disease. *Clin J Am Soc Nephrol* 2013; **8**: 1089-1097 [PMID: 23520042 DOI: 10.2215/CJN.10561012]

3 **Ong AC**, Devuyst O, Knebelmann B, Walz G; ERA-EDTA Working Group for Inherited Kidney Diseases. Autosomal dominant polycystic kidney disease: the changing face of clinical management. *Lancet* 2015; **385**: 1993-2002 [PMID: 26090645 DOI: 10.1016/S0140-6736(15)60907-2]

4 **Porath B**, Gainullin VG, Cornec-Le Gall E, Dillinger EK, Heyer CM, Hopp K, Edwards ME, Madsen CD, Mauritz SR, Banks CJ, Baheti S, Reddy B, Herrero JI, Bañales JM, Hogan MC, Tasic V, Watnick TJ, Chapman AB, Vigneau C, Lavainne F, Audrézet MP, Ferec C, Le Meur Y, Torres VE; Genkyst Study Group, HALT Progression of Polycystic Kidney Disease Group; Consortium for Radiologic Imaging Studies of Polycystic Kidney Disease, Harris PC. Mutations in GANAB, Encoding the Glucosidase Ⅱα Subunit, Cause Autosomal-Dominant Polycystic Kidney and Liver Disease. *Am J Hum Genet* 2016; **98**: 1193-1207 [PMID: 27259053 DOI: 10.1016/j.ajhg.2016.05.004]

5 **Harris PC**, Torres VE. Polycystic kidney disease. *Annu Rev Med* 2009; **60**: 321-337 [PMID: 18947299 DOI: 10.1146/annurev.med.60.101707.125712]

6 **Torres VE**. Therapies to slow polycystic kidney disease. *Nephron Exp Nephrol* 2004; **98**: e1-e7 [PMID: 15361692 DOI: 10.1159/000079926]

7 **Pei Y**, Watnick T. Diagnosis and screening of autosomal dominant polycystic kidney disease. *Adv Chronic Kidney Dis* 2010; **17**: 140-152 [PMID: 20219617 DOI: 10.1053/j.ackd.2009.12.001]

8 **Torres VE**, King BF, Chapman AB, Brummer ME, Bae KT, Glockner JF, Arya K, Risk D, Felmlee JP, Grantham JJ, Guay-Woodford LM, Bennett WM, Klahr S, Meyers CM, Zhang X, Thompson PA, Miller JP; Consortium for Radiologic Imaging Studies of Polycystic Kidney Disease (CRISP). Magnetic resonance measurements of renal blood flow and disease progression in autosomal dominant polycystic kidney disease. *Clin J Am Soc Nephrol* 2007; **2**: 112-120 [PMID: 17699395 DOI: 10.2215/CJN.00910306]

9 **Bae KT**, Tao C, Zhu F, Bost JE, Chapman AB, Grantham JJ, Torres VE, Guay-Woodford LM, Meyers CM, Bennett WM; Consortium for Radiologic Imaging Studies Polycystic Kidney Disease. MRI-based kidney volume measurements in ADPKD: reliability and effect of gadolinium enhancement. *Clin J Am Soc Nephrol* 2009; **4**: 719-725 [PMID: 19339416 DOI: 10.2215/CJN.03750708]

10 **Chapman AB**, Wei W. Imaging approaches to patients with polycystic kidney disease. *Semin Nephrol* 2011; **31**: 237-244 [PMID: 21784272 DOI: 10.1016/j.semnephrol.2011.05.003]

11 **Norman J**. Fibrosis and progression of autosomal dominant polycystic kidney disease (ADPKD). *Biochim Biophys Acta* 2011; **1812**: 1327-1336 [PMID: 21745567 DOI: 10.1016/j.bbadis.2011.06.012]

12 **Swenson-Fields KI**, Vivian CJ, Salah SM, Peda JD, Davis BM, van Rooijen N, Wallace DP, Fields TA. Macrophages promote polycystic kidney disease progression. *Kidney Int* 2013; **83**: 855-864 [PMID: 23423256 DOI: 10.1038/ki.2012.446]

13 **Mun H**, Park JH. Inflammation and Fibrosis in ADPKD. *Adv Exp Med Biol* 2016; **933**: 35-44 [PMID: 27730433 DOI: 10.1007/978-981-10-2041-4_4]

14 **Grantham JJ**, Cook LT, Torres VE, Bost JE, Chapman AB, Harris PC, Guay-Woodford LM, Bae KT. Determinants of renal volume in autosomal-dominant polycystic kidney disease. *Kidney Int* 2008; **73**: 108-116 [PMID: 17960141 DOI: 10.1038/sj.ki.5002624]

15 **Raman A**, Reif GA, Dai Y, Khanna A, Li X, Astleford L, Parnell SC, Calvet JP, Wallace DP. Integrin-Linked Kinase Signaling Promotes Cyst Growth and Fibrosis in Polycystic Kidney Disease. *J Am Soc Nephrol* 2017; **28**: 2708-2719 [PMID: 28522687 DOI: 10.1681/ASN.2016111235]

16 **Karihaloo A**, Li X. Role of Inflammation in Polycystic Kidney Disease. In: Li X, editor. Polycystic Kidney Disease. Brisbane (AU): Codon Publications, 2015: Chapter 14 [PMID: 27512776 DOI: 10.15586/codon.pkd.2015.ch14]

17 **Li JY**, Yong TY, Michael MZ, Gleadle JM. Review: The role of microRNAs in kidney disease. *Nephrology (Carlton)* 2010; **15**: 599-608 [PMID: 20883280 DOI: 10.1111/j.1440-1797.2010.01363.x]

18 **Patel V**, Noureddine L. MicroRNAs and fibrosis. *Curr Opin Nephrol Hypertens* 2012; **21**: 410-416 [PMID: 22622653 DOI: 10.1097/MNH.0b013e328354e559]

19 **Patel V**, Williams D, Hajarnis S, Hunter R, Pontoglio M, Somlo S, Igarashi P. miR-17~92 miRNA cluster promotes kidney cyst growth in polycystic kidney disease. *Proc Natl Acad Sci U S A* 2013; **110**: 10765-10770 [PMID: 23759744 DOI: 10.1073/pnas.1301693110]

20 **Hajarnis SS**, Patel V, Aboudehen K, Attanasio M, Cobo-Stark P, Pontoglio M, Igarashi P. Transcription Factor Hepatocyte Nuclear Factor-1β (HNF-1β) Regulates MicroRNA-200 Expression through a Long Noncoding RNA. *J Biol Chem* 2015; **290**: 24793-24805 [PMID: 26292219 DOI: 10.1074/jbc.M115.670646]

21 **Lakhia R**, Hajarnis S, Williams D, Aboudehen K, Yheskel M, Xing C, Hatley ME, Torres VE, Wallace DP, Patel V. MicroRNA-21 Aggravates Cyst Growth in a Model of Polycystic Kidney Disease. *J Am Soc Nephrol* 2016; **27**: 2319-2330 [PMID: 26677864 DOI: 10.1681/ASN.2015060634]

22 **Liang M**, Liu Y, Mladinov D, Cowley AW Jr, Trivedi H, Fang Y, Xu X, Ding X, Tian Z. MicroRNA: a new frontier in kidney and blood pressure research. *Am J Physiol Renal Physiol* 2009; **297**: F553-F558 [PMID: 19339633 DOI: 10.1152/ajprenal.00045.2009]

23 **Wahid F**, Shehzad A, Khan T, Kim YY. MicroRNAs: synthesis, mechanism, function, and recent clinical trials. *Biochim Biophys Acta* 2010; **1803**: 1231-1243 [PMID: 20619301 DOI: 10.1016/j.bbamcr.2010.06.013]

24 **Alberti C**, Cochella L. A framework for understanding the roles of miRNAs in animal development. *Development* 2017; **144**: 2548-2559 [PMID: 28720652 DOI: 10.1242/dev.146613]

25 **Christopher AF**, Kaur RP, Kaur G, Kaur A, Gupta V, Bansal P. MicroRNA therapeutics: Discovering novel targets and developing specific therapy. *Perspect Clin Res* 2016; **7**: 68-74 [PMID: 27141472 DOI: 10.4103/2229-3485.179431]

26 **Vettori S**, Gay S, Distler O. Role of MicroRNAs in Fibrosis. *Open Rheumatol J* 2012; **6**: 130-139 [PMID: 22802911 DOI: 10.2174/1874312901206010130]

27 **Lantinga-van Leeuwen IS**, Dauwerse JG, Baelde HJ, Leonhard

WN, van de Wal A, Ward CJ, Verbeek S, Deruiter MC, Breuning MH, de Heer E, Peters DJ. Lowering of Pkd1 expression is sufficient to cause polycystic kidney disease. *Hum Mol Genet* 2004; **13**: 3069-3077 [PMID: 15496422 DOI: 10.1093/hmg/ddh336]

28 **Tan YC**, Blumenfeld J, Rennert H. Autosomal dominant polycystic kidney disease: genetics, mutations and microRNAs. *Biochim Biophys Acta* 2011; **1812**: 1202-1212 [PMID: 21392578 DOI: 10.1016/j.bbadis.2011.03.002]

29 **Patel V**, Hajarnis S, Williams D, Hunter R, Huynh D, Igarashi P. MicroRNAs regulate renal tubule maturation through modulation of Pkd1. *J Am Soc Nephrol* 2012; **23**: 1941-1948 [PMID: 23138483 DOI: 10.1681/ASN.2012030321]

30 **Hajarnis S**, Lakhia R, Yheskel M, Williams D, Sorourian M, Liu X, Aboudehen K, Zhang S, Kersjes K, Galasso R, Li J, Kaimal V, Lockton S, Davis S, Flaten A, Johnson JA, Holland WL, Kusminski CM, Scherer PE, Harris PC, Trudel M, Wallace DP, Igarashi P, Lee EC, Androsavich JR, Patel V. microRNA-17 family promotes polycystic kidney disease progression through modulation of mitochondrial metabolism. *Nat Commun* 2017; **8**: 14395 [PMID: 28205547 DOI: 10.1038/ncomms14395]

31 **Xu X**, Kriegel AJ, Liu Y, Usa K, Mladinov D, Liu H, Fang Y, Ding X, Liang M. Delayed ischemic preconditioning contributes to renal protection by upregulation of miR-21. *Kidney Int* 2012; **82**: 1167-1175 [PMID: 22785173 DOI: 10.1038/ki.2012.241]

32 **Kriegel AJ**, Liu Y, Liu P, Baker MA, Hodges MR, Hua X, Liang M. Characteristics of microRNAs enriched in specific cell types and primary tissue types in solid organs. *Physiol Genomics* 2013; **45**: 1144-1156 [PMID: 24085797 DOI: 10.1152/physiolgenomics.00090.2013]

33 **Kriegel AJ**, Baker MA, Liu Y, Liu P, Cowley AW Jr, Liang M. Endogenous microRNAs in human microvascular endothelial cells regulate mRNAs encoded by hypertension-related genes. *Hypertension* 2015; **66**: 793-799 [PMID: 26283043 DOI: 10.1161/HYPERTENSIONAHA.115.05645]

34 **Harris PC**, Torres VE. Genetic mechanisms and signaling pathways in autosomal dominant polycystic kidney disease. *J Clin Invest* 2014; **124**: 2315-2324 [PMID: 24892705 DOI: 10.1172/JCI72272]

35 **Liu Y**. Renal fibrosis: new insights into the pathogenesis and therapeutics. *Kidney Int* 2006; **69**: 213-217 [PMID: 16408108 DOI: 10.1038/sj.ki.5000054]

36 **Wei J**, Besner GE. M1 to M2 macrophage polarization in heparin-binding epidermal growth factor-like growth factor therapy for necrotizing enterocolitis. *J Surg Res* 2015; **197**: 126-138 [PMID: 25913486 DOI: 10.1016/j.jss.2015.03.023]

37 **Harskamp LR**, Gansevoort RT, Boertien WE, van Oeveren W, Engels GE, van Goor H, Meijer E. Urinary EGF Receptor Ligand Excretion in Patients with Autosomal Dominant Polycystic Kidney Disease and Response to Tolvaptan. *Clin J Am Soc Nephrol* 2015; **10**: 1749-1756 [PMID: 26231191 DOI: 10.2215/CJN.09941014]

38 **Harskamp LR**, Gansevoort RT, van Goor H, Meijer E. The epidermal growth factor receptor pathway in chronic kidney diseases. *Nat Rev Nephrol* 2016; **12**: 496-506 [PMID: 27374915 DOI: 10.1038/nrneph.2016.91]

39 **Talbot JJ**, Shillingford JM, Vasanth S, Doerr N, Mukherjee S, Kinter MT, Watnick T, Weimbs T. Polycystin-1 regulates STAT activity by a dual mechanism. *Proc Natl Acad Sci U S A* 2011; **108**: 7985-7990 [PMID: 21518865 DOI: 10.1073/pnas.1103816108]

40 **Talbot JJ**, Song X, Wang X, Rinschen MM, Doerr N, LaRiviere WB, Schermer B, Pei YP, Torres VE, Weimbs T. The cleaved cytoplasmic tail of polycystin-1 regulates Src-dependent STAT3 activation. *J Am Soc Nephrol* 2014; **25**: 1737-1748 [PMID: 24578126 DOI: 10.1681/ASN.2013091026]

41 **Meng J**, Li L, Zhao Y, Zhou Z, Zhang M, Li D, Zhang CY, Zen K, Liu Z. MicroRNA-196a/b Mitigate Renal Fibrosis by Targeting TGF-β Receptor 2. *J Am Soc Nephrol* 2016; **27**: 3006-3021 [PMID: 26940097 DOI: 10.1681/ASN.2015040422]

42 **Wynn TA**, Ramalingam TR. Mechanisms of fibrosis: therapeutic translation for fibrotic disease. *Nat Med* 2012; **18**: 1028-1040 [PMID: 22772564 DOI: 10.1038/nm.2807]

P- Reviewer: Chang CC, Rangan G **S- Editor**: Wang JL
L- Editor: Filipodia **E- Editor**: Song H

Published by **Baishideng Publishing Group Inc**
7901 Stoneridge Drive, Pleasanton, CA 94588, USA
Telephone: +1-925-223-8242
Fax: +1-925-223-8243
E-mail: bpgoffice@wjgnet.com
Help Desk: http://www.f6publishing.com/helpdesk
http://www.wjgnet.com

© 2018 Baishideng Publishing Group Inc. All rights reserved.